UNIVERSITY OF CRETE
DEPARTMENT OF PHYSICS

Master Thesis

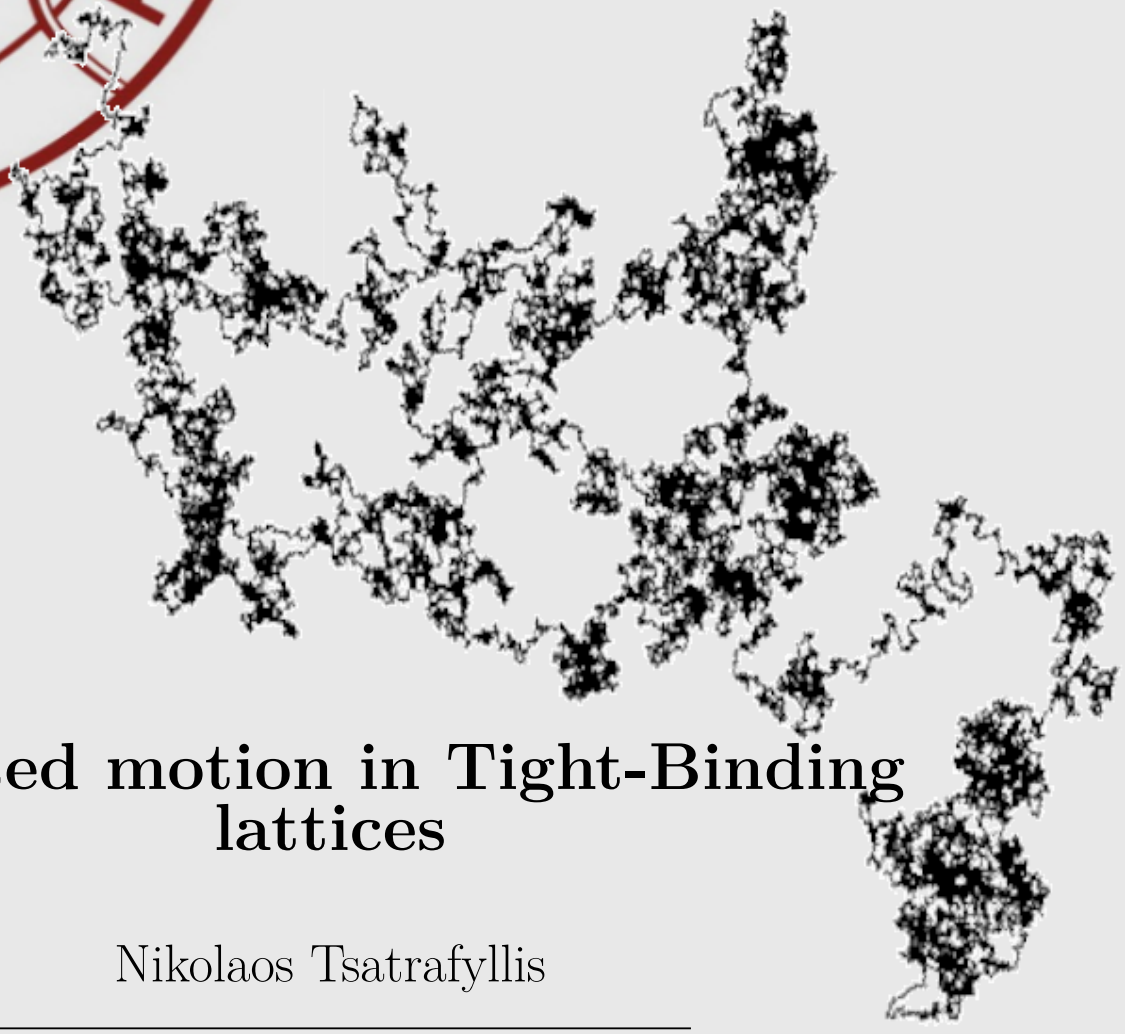

Directed motion in Tight-Binding lattices

Nikolaos Tsatrafyllis

Advisor: *Prof.* Giorgos Tsironis - University of Crete

UNIVERSITY OF CRETE
DEPARTMENT OF PHYSICS

MSc THESIS

IN

- CONDENSED MATTER PHYSICS -

Defended by

NIKOLAOS TSATRAFYLLIS

Directed motion in Tight Bindind lattices

COMMITTEE

Prof.	Giorgos Tsironis	-	UNIVERSITY OF CRETE
Prof.	Xenophon Zotos	-	UNIVERSITY OF CRETE
Prof.	Nikos Flytzanis	-	UNIVERSITY OF CRETE

Date of the defense:
03/09/2013

Abstract

Classical directed motion and quantum diffusion for a particle are studied in one-dimension. In the Classical regime, we examined through stochastic simulations in the Langevin picture the motion of an over-damped Brownian particle in a periodic, non-symmetric *ratchet* potential driven by time-correlated forces. We focused on two extreme limits, the *white noise limit* where the correlation time goes to zero, where we found numerically that white uncorrelated fluctuations cannot induce macroscopic current. In the other extreme limit when the correlation time is very large, we noticed that the time correlations of the noise can create a non zero current due to the asymmetry of the potential, the well-known *Ratchet effect*. In the quantum regime we studied the motion of a charged particle through the stochastic Liouville equation, using analytical as well as numerical means, in three different one - dimensional discrete tight-binding lattices : (i) the single-band, (ii) the two-band and (iii) the tree-band lattice, in the presence/absence of a sinusoidal electric field. Additionally, the coupling of the charged particle to the environment was taken into account in a phenomenological way by adding proper terms in the Liouville equation. Quantum diffusion can been seen in all cases except for the very special case of the linear lattice with an AC drive, where *dynamic localization* appears for special values of the electric field's parameters. The phenomenon of dynamic localization, for the same parameter regime disappears for the other types of lattices.

Acknowledgements

First of all, I would like to show my gratitude to my supervisor prof. Giorgos Tsironis, for introducing me into the physics of non-linear phenomena and I am grateful for his guidance and trust during this work. I would also like to thank Nikos Lazarides who was always there to listen and help.

This thesis would not have been possible without the support, help and the endless scientific discussions of my colleagues and friends Christina Psaroudaki and Yannis Iatrakis.

Last but not least, I would like to thank my friends Stergios Kyanidis, Alexandra Roussou and Joniald Shena for their moral support, and their efforts to keep me calm and concentrated during hard days when everything seemed to go extremely wrong.

Contents

List of Figures **xi**

1 Introduction **1**

1.1 Brownian Motion 1

1.1.1 Langevin Equations 1

1.2 Open Quantum System Dynamics 3

1.2.1 Lindblad Master Equation 3

1.2.2 Stochastic Liouville Equation 3

1.3 Ratchets 4

2 Classical Motion **5**

2.1 Introduction 5

2.2 Basic Method 6

2.3 The *Ratchet Effect* 7

2.3.1 Small Correlation Time $\tau \to 0$ 8

2.3.2 Large Correlation Time $\tau \gg 1$ 9

3 Quantum Motion In a Closed System **11**

3.1 Introduction 11

3.2 1-D Discrete One-Band Lattice 12

3.2.1 Absence of Electric Field 12

3.2.2 Presence of Electric Field 16

3.3 1-D Discrete Two-Band Lattice 22

3.3.1 Absence of Electric Field 23

3.3.2 Presence of Electric Field 24

3.4 1-D Discrete Three-Band Lattice 26

3.4.1 Absence of Electric Field 27

3.4.2 Presence of Electric Field 28

4 Quantum Motion In an Open System **31**

4.1 Introduction 31

4.2 1-D Discrete One-Band Lattice 32

4.2.1 Absence of Electric Field 32

4.2.2 Presence of Electric Field 36

4.3 1-D Discrete Two-Band Lattice 40

4.3.1 Absence of Electric Field 40

4.3.2 Presence of Electric Field 41

4.4 1-D Discrete Three-Band Lattice 43

4.4.1 Absence of Electric Field 44

4.4.2 Presence of Electric Field 45

5 Discussion **47**

Bibliography **51**

List of Figures

2.1 (a) Asymmetric ratchet potential and (b) Asymmetric ratchet force (Langevin force), for height Q=1, period L=1 and asymmetry parameter b=0.5 . 7

2.2 The mean value of position, plotted as a function of time four different realizations N. The red solid line corresponds to $N = 100$, the green solid line corresponds to $N = 500$, the purple solid line corresponds to $N = 1000$ and the blue solid line corresponds to $N = 2000$. As the realizations increase, the result becomes more accurate and we obtain $\langle x \rangle(t) \to 0$. As a consequence, a net current does not appear. 9

2.3 The mean value of position, plotted as a function of time four different realizations N. The red solid line corresponds to $N = 100$, the green solid line corresponds to $N = 500$, the purple solid line corresponds to $N = 1000$ and the blue solid line corresponds to $N = 2000$.. As the realizations increase, the result becomes more accurate and the $\langle x \rangle(t) \neq 0$. From this graph it is clear that a ratchet current appears. 10

3.1 Quantum motion of a particle in 1-D discrete one-band lattice of l sites, with the electic field set to zero. 12

3.2 Quantum motion of a particle in 1-D discrete one-band lattice of l sites, under the presence of time-dependent (AC) electric field. 17

3.3 The mean square displacement, plotted as a function of time for different values of the ratio $\mathscr{E}_0/\omega$ for an AC field, whereas the ratio $\mathscr{E}_0/V$ is constant and equals 5. (a) $\mathscr{E}_0/\omega = 0$, (b) $\mathscr{E}_0/\omega = 1$, (c) $\mathscr{E}_0/\omega = 3$ and (d) $\mathscr{E}_0/\omega = 2.405$, which is the first root of $J_0(\mathscr{E}_0/\omega = 2.405)$ and shows the well known phenomenon of dynamic localization. The blue solid line corresponds to analytical solution, whereas the black dashed line corresponds to our numerical simulations. 22

3.4 Quantum motion of a particle in 1-D discrete two-band lattice of l sites, in the absence of electric field. The two bands, have an energy difference 2ϵ. 23

3.5 The numerical simulation of mean square displacement, plotted as a function of time for the 1-D discrete two-band lattice. The blue solid line corresponds to our numerical results and the black dashed line corresponds to best fit of our data. 24

3.6 Quantum motion of a particle in 1-D discrete two-band lattice of l sites, in the presence of time-dependent (AC) electric field. 25

3.7 The numerical simulation of mean square displacement, plotted as a function of time for the 1-D discrete two-band lattice in presence of a sinusoidal electric field, for different values of the ratio $\mathscr{E}_0/\omega$. The ratio $\mathscr{E}_0/V$ is constant and equals 5. (a) $\mathscr{E}_0/\omega = 1$, (b) $\mathscr{E}_0/\omega = 3$, (c) $\mathscr{E}_0/\omega = 2.405$. We notice here, the disappearance of the dynamic localization phenomenon, for the value $\mathscr{E}_0/\omega = 2.405$. 26

3.8 Quantum motion of a particle in 1-D discrete three-band lattice of l sites, in the absence of electric field. The three bands, have a minimum energy difference 2ϵ and a maximum 4ϵ. The index l denotes the first band, $l+1$ the second an $l+2$ the third one. 27

3.9 The numerical simulation of mean square displacement, plotted as a function of time for the 1-D discrete three-band lattice. The blue solid line corresponds to our numerical results and the black dashed line corresponds to best fit of our data. 28

3.10 Quantum motion of a particle in 1-D discrete three-band lattice of l sites, in the presence of time-dependent (AC) electric field. 29

3.11 The numerical simulation of mean square displacement, plotted as a function of time for the 1-D discrete three-band lattice in presence of a sinusoidal electric field, for different values of the ratio $\mathscr{E}_0/\omega$. The ratio $\mathscr{E}_0/V$ is constant and equals 5. (a) $\mathscr{E}_0/\omega = 1$, (b) $\mathscr{E}_0/\omega = 3$, (c) $\mathscr{E}_0/\omega = 2.405$. The phenomenon of dynamic localization does not appear for these parameter values. 30

4.1 The mean square displacement, plotted as a function of time. (a) $\alpha/\omega = 15$ and $\alpha/\mathscr{E}_0 = 0.1$, (b) $\alpha/\omega = 15$ and $\alpha/\mathscr{E}_0 = 0.2$, (c) $\alpha/\omega = 0.15$ and $\alpha/\mathscr{E}_0 = 0.1$, and (d) $\alpha/\omega = 0.15$ and $\alpha/\mathscr{E}_0 = 0.2$.The main behavior of MSD is proportional to time. 39

4.2 The numerical simulation of mean square displacement, plotted as a function of time for the 1-D discrete two-band lattice in the presence of the coupling of the charged particle with the environment($\alpha = 0.5$). We note here, that the MSD $\propto$ t. The blue solid line corresponds to our numerical results and the black dashed line corresponds to best fit of our data. 41

4.3 The mean square displacement, plotted as a function of time. (a) $\alpha/\omega = 15$ and $\alpha/\mathscr{E}_0 = 0.1$, (b) $\alpha/\omega = 15$ and $\alpha/\mathscr{E}_0 = 0.2$, (c) $\alpha/\omega = 0.15$ and $\alpha/\mathscr{E}_0 = 0.1$, and (d) $\alpha/\omega = 0.15$ and $\alpha/\mathscr{E}_0 = 0.2$. 43

4.4 The numerical simulation of mean square displacement, plotted as a function of time for the 1-D discrete three-band lattice in the presence of the coupling of the charged particle with the environment. The blue solid line corresponds to our numerical results and the black dashed line corresponds to best fit of our data. 45

4.5 The mean square displacement, plotted as a function of time. (a) $\alpha/\omega = 15$ and $\alpha/\mathscr{E}_0 = 0.1$, (b) $\alpha/\omega = 15$ and $\alpha/\mathscr{E}_0 = 0.2$, (c) $\alpha/\omega = 0.15$ and $\alpha/\mathscr{E}_0 = 0.1$, and (d) $\alpha/\omega = 0.15$ and $\alpha/\mathscr{E}_0 = 0.2$. 46

List of Figures

1 Introduction

1.1 Brownian Motion

The theory of Brownian motion deals with the random motion of small particles suspended in a fluid (a liquid or a gas) resulting from their bombardment by the fast-moving atoms or molecules in the gas or liquid; this theory provides an idealized approximate way to treat the dynamics of non equilibrium systems. Brownian motion is among the simplest of the continuous-time stochastic (or probabilistic) processes, and it is a limit of both simpler and more complicated stochastic processes. The fundamental equation describing such motion is called the Langevin equation. This equation contains both frictional forces and random forces, which are related to each other through the fluctuation-dissipation theorem (FDT).

1.1.1 Langevin Equations

While the motion of a particle performing Brownian motion appears to be quite random, it must nevertheless be describable by the same equation of motion as is any other dynamical systems, e.g. in classical mechanics these are Newton's or Hamilton's equations. Hence, let us consider the classical motion of a particle, for simplicity in one

dimension, described by the Newton's second law of motion :

$$m\frac{d}{dt}u(t) = F(t) \tag{1.1}$$

where $F(t)$ is the total force describing the interaction of the Brownian particle with the surrounding medium at time t. If the positions of the molecules in the surrounding medium were already known as a function of time, then in principle this force is a known function of time. In this sense it is not a random force at all. Usually, it is not practical or even desirable to look for an exact expression of $F(t)$. This force is most frequently represented by a friction force proportional to velocity (Stokes' force) of the Brownian particle, i.e. $-\gamma u(t)$, where γ is given by Stokes' law:

$$\gamma = 6\pi\eta r \tag{1.2}$$

where η is the viscosity of the fluid medium and r is the particle's radius. We also expect a random force $\xi(t)$ due to random density fluctuations in the fluid, representing the effect of the collisions with the molecules of the fluid (noise term). Defining $\tau = m/\gamma$ as the relaxation time of the macroscopic motion of the particle, the equations of motion of the Brownian particle are:

$$\begin{aligned} \frac{d}{dt}x(t) &= u(t) \\ \frac{d}{dt}u(t) &= -\frac{1}{\tau}u(t) + \frac{1}{m}\xi(t) \end{aligned} \tag{1.3}$$

These are the *Langevin equations* of motion for the Brownian particle.

For Eqs (1.3) to be meaningful we must specify the statistical properties of the random force $\xi(t)$; we assume that it is correlated at a very small time compared to the relaxation time of the system. An idealized case is to assume that the random force has zero correlation time, so $\xi(t)$ is approximated by a δ-correlated process [1]:

$$\begin{aligned} \langle\xi(t)\rangle &= 0 \\ \langle\xi(t)\xi(t')\rangle &= 2D\delta(t-t') \end{aligned} \tag{1.4}$$

which means that, all the frequencies of its power spectrum have equal weight.

1.2 Open Quantum System Dynamics

An open quantum system is a quantum system which is found to be in interaction with an external quantum system, the environment. The theory of open quantum systems addresses the problems of damping and dephasing in quantum systems by the assertion that all real systems of interest are "open" systems (surrounded by their environments). In general, the quantum dynamics of open quantum systems cannot be represented by a unitary time evolution. In many cases, it is useful to formulate the dynamics of such quantum systems by an appropriate equation of motion for their density matrix, i.e. a quantum master equation.

1.2.1 Lindblad Master Equation

The simplest case representing these dynamics is the quantum Markov processes [2], a first-order linear differential equation for the reduced density matrix, defined by:

$$\dot{\rho} = -\frac{i}{\hbar}[H,\rho] - \sum_k \gamma_k (L_k \rho L_k^\dagger - \frac{1}{2}\left(\rho L_k^\dagger L_k + L_k^\dagger L_k \rho\right)) \tag{1.5}$$

which is known as *quantum Markovian master equation in Lindblad form.* If only the first term existed, in the right-hand side of Eq. (1.5), is the *Liouville-von Neumann equation* which is the usual shrödinger term that generates unitary evolution. The other terms describe the possible transitions that the system may undergo due to interactions with the reservoir. The operators L_k are called Lindblad operators, while the γ_k are correlation functions of the reservoir.

1.2.2 Stochastic Liouville Equation

Since Kubo's work [3–5] on a random frequency modulation model for nuclear magnetic resonance (NMR) published in 1954, and later in 1962 on transport equations, the stochastic theory has been proven to be useful for studying various topics in physics.

The well-known stochastic model describes perturbation in the Zeeman energy of a spin by a local random field that originates from dipolar interactions of many other spins in the environment. Such perturbation that causes random formation can be

regarded as a stochastic process. He used an effective Hamiltonian $H(t)$ for the spin as a function of stochastic variables $\Omega(t)$ which represents the states of the environment:

$$H(t) = H_0(t) + H_1(\Omega(t)) \tag{1.6}$$

where $H_0(t)$ is th unpertubed Hamiltonian and $H_1(\Omega(t))$ is the stochastic perturbation.

Thus, the density matrix elements of a spin system become a function of the spin state and stochastic variable. The time evolution of the spin state follows the quantum Liouville equation, whereas the stochastic variables follow a certain law of stochastic time evolution. This type of approach called a stochastic approach in contrast to a dynamical approach. The stochastic approach has been used repeatedly to treat dynamical systems under the influence of their environment, where if the characteristic time of the main system is much longer than that of the bath, one can regard that the bath interaction is a Markovian process. Therefore the reduced density matrix equations of motion has the same form to the stochastic Liouville equation.

1.3 Ratchets

Thermal ratchets, also known as Brownian ratchets are over-damped systems that transport Brownian particles with nonzero macroscopic velocity along one-dimensional asymmetric periodic structures due to the effect of non equilibrium fluctuations, although on average no macroscopic force is acting. Ratchet systems have found diverse applications in many areas, from mechanical devices up to quantum systems and it is believed that various biological motion can be explained by the function of tiny motor proteins operating at the molecular scale using the ratchet effect [6, 7].

2 Classical Motion

2.1 Introduction

When a microtubular associated protein (MAP) executes motion on a microtubule, its diffusive dynamics has a specified directed motion. This phenomenon, as commonly called *Ratchet Effect* has been the focus of attention of many physicists for many years. Although, in essence the origin of this effect was biological, it was a challenge for physicists to understand the mechanism of motor protein motion, therefore they began to study several ratchet models, such as the over-damped particles in a periodic but nonsymmetric potentials, Figure 2.1, driven by different correlated noises [8]. This model leads to a Brownian particle, moving in a specific direction determined by the potential asymmetry and the properties of a noise. In this Chapter, we will consider an over-damped particle under the influence of two forces, (i) a spatial asymmetrical periodic force (ratchet force) $f(x)$ resulted from the potential $f(x) = -\frac{d}{dx}V(x)$ and (ii) a random time-periodic force $\xi(t)$ as a consequence of the coupling of the particle with the environment. The equation of motion which the particle obeys has the form:

$$\frac{dx(t)}{dt} = f(x) + \xi(t) \tag{2.1}$$

where $\xi(t)$ is defined by

$$\frac{d\xi(t)}{dt} = \frac{\eta(t) - \xi(t)}{\tau} \tag{2.2}$$

where $\eta(t)$ is a δ - correlated Gaussian noise of any non zero correlation time τ. We present numerical results by solving Eq.(2.1) N times for different realizations and plotting

$$\langle x \rangle(t) = \frac{1}{N} \sum_n x_n \tag{2.3}$$

and we show the onset of *Ratchet Effect* for large correlation times; this phenomenon does not hold for small correlation times as expected, as the rates of escape to the left or to the right become equal [9, 10].

2.2 Basic Method

In this section we introduce the mathematical tools for studying the stochastic motion of a particle in a periodic but non symmetric potential, coupled with the environment. The most direct way of implementing this Brownian motion is to recognize that there is a stochastic component to the force on the particle, which we only know through a probabilistic description. This process is described by the Langevin equation for the position $x(t)$.

$$\begin{aligned} \frac{dx(t)}{dt} &= f(x) + \xi(t) \\ \frac{d\xi(t)}{dt} &= \frac{\eta(t) - \xi(t)}{\tau} \end{aligned} \tag{2.4}$$

Here $x(t)$ denotes the position of the Brownian particle, while $f(x) = -\frac{d}{dx}V(x)$ denotes the spatial asymmetrical and periodic force which acts on the particle, caused by the potential $V(x)$ which we have submitted (Figure 2.1). The variable ξ represents the coupling of the particle with the environment and $\eta(t)$ the noise variable, which is Gaussian and δ-correlated,i.e

$$\langle \eta(t)\eta(t') \rangle = D\delta(t - t') \tag{2.5}$$

where D is the noise intensity. Then the variable $\xi(t)$ is an Ornstein-Uhlenbeck (O-U) process, which means that $\xi(t)$ is Gaussian and exponentially correlated.

$$\langle \xi(t)\xi(t') \rangle = \frac{D}{2\tau} e^{-|t-t'||/\tau} \tag{2.6}$$

and τ is the correlation time. The potential [10] in the figure is defined as follows:

$$V(x) \quad = \quad \frac{1}{2} Q \left(1 + \frac{sin(2\pi x/L - \phi_c) + bsin[2(2\pi x/L - \phi_c)]}{sin(\phi_c) + bsin(2\phi_c)} \right) \tag{2.7}$$

where $\phi_c = arcos[(-1 + \sqrt{1 + 32b^2})/8b]$. This is a potential of height Q, period L and asymmetry b. We should remark here that for $b < 0.5$ the potential has one maximum and one minimum within a period, while for $b > 0.5$ a second minimum and maximum appear, but it is still asymmetric. Thus, the most asymmetric form of the potential is for $b = 0.5$.

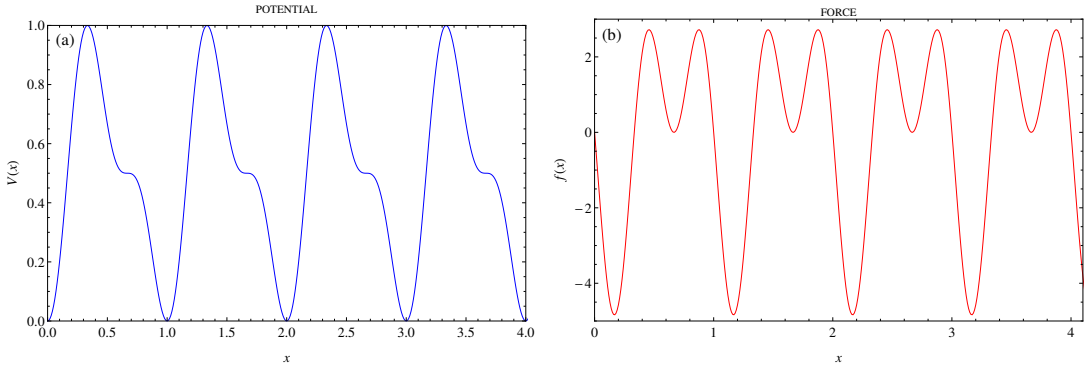

Figure 2.1: (a) Asymmetric ratchet potential and (b) Asymmetric ratchet force (Langevin force), for height Q=1, period L=1 and asymmetry parameter b=0.5

We are now in a position to describe the *Ratchet Effect* by solving Eq.(2.4) numerically, N times for different realizations of the colored noise $\xi(t)$, by computing and plotting the mean value of position, as a function of position Eq. (2.3).

2.3 The *Ratchet Effect*

The numerical calculation of the mean value of the position was done for two limits of correlation time τ. For this reason, the section is separated in two subsections. The

first subsection, includes numerical calculations for small correlation time ($\tau \to 0$), i.e white noise, whereas in the second one, we present numerical calculations for large correlation time ($\tau \gg 1$), i.e colored noise, where the *Ratchet Effect* appears.

2.3.1 Small Correlation Time $\tau \to 0$

We consider the motion of an over-damped particle moving under the influence of a periodic but non symmetric force, coupled with the environment as described above, in the limit $\tau \to 0$ (white noise limit), where we do not expected to observe a macroscopic current. Thus, we solve the Langevin equation (Eq. 2.4) numerically N times, for different realizations of the white noise. More specifically, the numerical calculations were made for $N = 100$, 500, 1000 and2000 realizations, while the strength of the noise D was kept constant, equal to 2. Finally, the potential parameter values are $Q = 1$, $L = 1$ and $b = 0.5$. The graph that follows below, Figure 2.2, demonstrates the mean value of position as a function of time, where it is shown that the $\langle x \rangle(t) = 0$, as we expected.

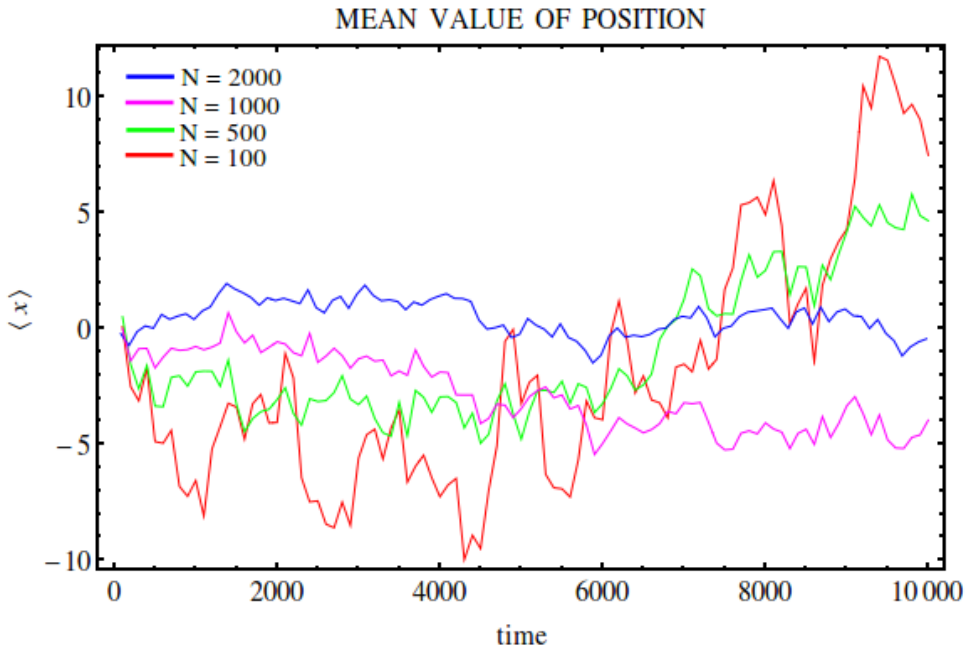

Figure 2.2: The mean value of position, plotted as a function of time four different realizations N. The red solid line corresponds to $N = 100$, the green solid line corresponds to $N = 500$, the purple solid line corresponds to $N = 1000$ and the blue solid line corresponds to $N = 2000$. As the realizations increase, the result becomes more accurate and we obtain $\langle x \rangle(t) \to 0$. As a consequence, a net current does not appear.

2.3.2 Large Correlation Time $\tau \gg 1$

Now we assume the same motion of a particle with the main difference that, our calculations made for very large correlation time, $\tau \gg 1$ (colored noise). The results presented below (Figure 2.3), where we plot again the mean value of position as a function of time. The numerical calculations made as before using the same features.

In this limit, when $\tau \gg 1$, in a thermodynamic sense, the system is open and a non-zero net current appears. The effect of white noise is negligible, thus $\dot{\xi}(t) \approx 0$, so approximately the force which acts in the particle is static, i.e. $f + \xi$, although ξ is fluctuating but very slowly. When ξ takes the value which cancels the *ratchet force*, the Brownian particle moves to the next well (in our case to the left, but this is not necessary) and so on.

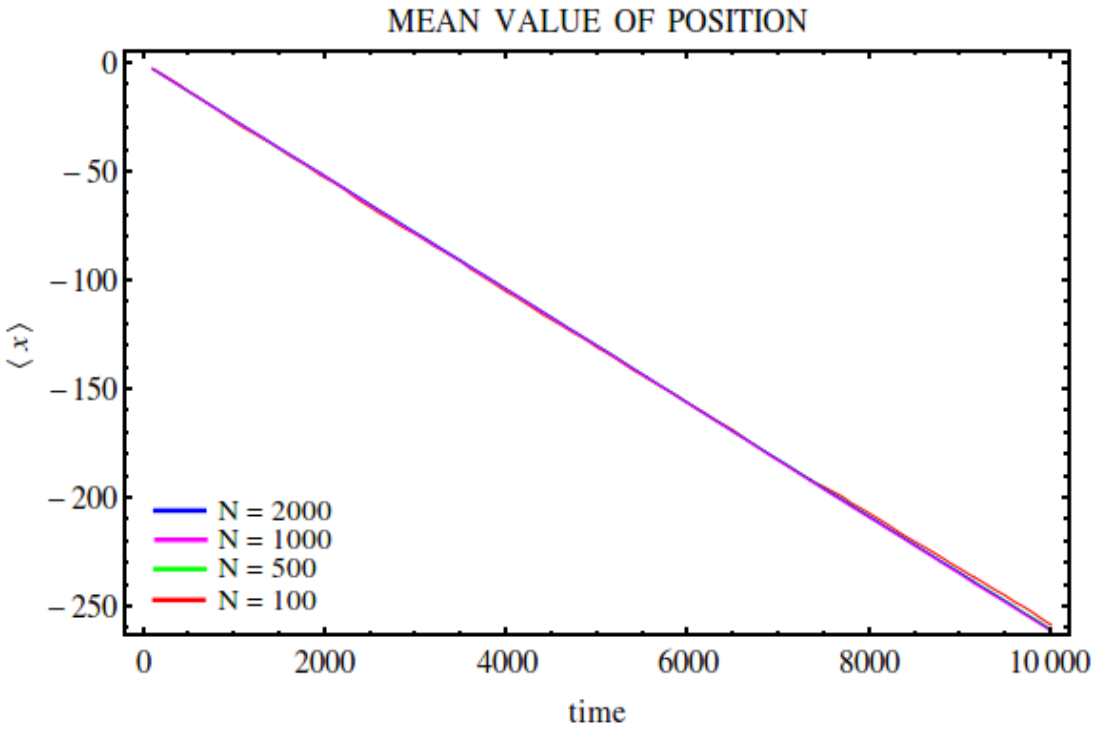

Figure 2.3: The mean value of position, plotted as a function of time four different realizations N. The red solid line corresponds to $N = 100$, the green solid line corresponds to $N = 500$, the purple solid line corresponds to $N = 1000$ and the blue solid line corresponds to $N = 2000$.. As the realizations increase, the result becomes more accurate and the $\langle x \rangle(t) \neq 0$. From this graph it is clear that a ratchet current appears.

3 Quantum Motion In a Closed System

3.1 Introduction

In this chapter, we consider the quantum motion of a charged particle moving on a one-dimensional discrete lattice of N sites under a Tight-Binding Hamiltonian,in the presence/absence of a time-dependent (sinusoidal) electric field, for three different cases. In the first section, we study the case of the quantum motion in a discrete one-band lattice where all on-site energies are the same. We obtain exact solutions for the mean square displacement (**MSD**), by solving the Liouville-von Neumann equation (**LVN**) of the form:

$$i\frac{\partial}{\partial t}\rho_{m,n} = V(\rho_{m+1,n} + \rho_{m-1,n} - \rho_{m,n+1} - \rho_{m,n-1}) + \mathscr{E}_0 f(t)(m-n)\rho_{m,n} \tag{3.1}$$

for $\mathscr{E}_0 = 0$ and $\mathscr{E}_0 \neq 0$. Eq. (3.1) can also be solved numerically, and the analytical and numerical results for the MSD can be compared for certain values of the electric field's frequency ω. Subsequently, we study numerically the quantum motion in discrete two-band lattice where two different on-site energies exist. This is performed by adding an on-site energy, at every second site. Therefore, we construct a lattice with two-bands,

where each band has different energy. This, can be expressed by an extra term in the LVN as follows:

$$i\frac{\partial}{\partial t}\rho_{m,n} = V(\rho_{m+1,n}+\rho_{m-1,n}-\rho_{m,n+1}-\rho_{m,n-1})+\mathscr{E}_0 f(t)(m-n)\rho_{m,n} + (\varepsilon_m-\varepsilon_n)\rho_{m,n} \quad (3.2)$$

From Eq. (3.2) we derive numerically the MSD as a function of time, with and without the term of the electric field, for different values of ω. Finally, we "break the symmetry", by separating the lattice in a three-band lattice following the same procedure as in the previous section. The equation which describes such a quantum motion is the same, as Eq.(3.2).

3.2 1-D Discrete One-Band Lattice

First, let us consider, the simplest and most trivial case of quantum motion of a charged particle e, moving on a discrete one-band 1-D lattice of sites l ($-\infty < l < \infty$) in absence of on-site energy [11].

3.2.1 Absence of Electric Field

In the case of a zero electric field (Figure 3.1) the Tight-Binding Hamiltonian is :

$$H^0 = V\sum_l |l\rangle\langle l+1| + |l+1\rangle\langle l| \quad (3.3)$$

where V is the nearest-neighbor intersite interactions (overlap integrals), and $|l\rangle$ represents a Wannier state localized on lattice site l. Expressing the charged particle state

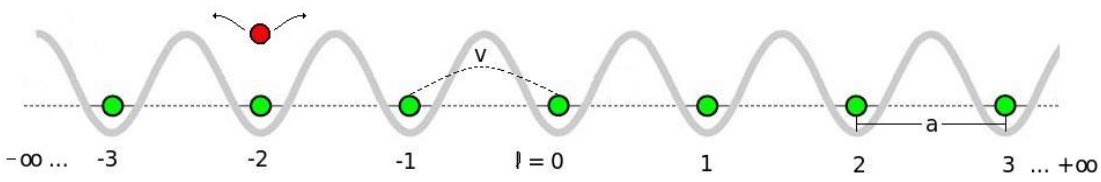

Figure 3.1: Quantum motion of a particle in 1-D discrete one-band lattice of l sites, with the electic field set to zero.

$|\Psi(t)\rangle$ as linear combination of Wannier states:

$$|\Psi(t)\rangle = \sum_i c_i(t)|i\rangle \quad and \quad \langle\Psi(t)| = \sum_j c_j^*(t)\langle j| \tag{3.4}$$

and using the Liouville-Von Neumann equation, we get the evolution equation for the density matrix:

$$i\frac{\partial}{\partial t}\rho(t) = [H^0, \rho(t)] \qquad (\hbar = 1) \tag{3.5}$$

where by definition:

$$\rho(t) = |\Psi(t)\rangle\langle\Psi(t)| = \sum_{i,j} c_i(t)c_j^*(t)|i\rangle\langle j| \tag{3.6}$$

From equations (3.4), (3.5) and (3.6), one obtains :

$$\begin{aligned} i\frac{\partial}{\partial t}(\sum_{i,j} c_i(t)c_j^*(t)|i\rangle\langle j|) &= V\sum_{i,j,l} c_i(t)c_j^*(t)(|l\rangle\langle l+1|i\rangle\langle j| + |l+1\rangle\langle l|i\rangle\langle j| - \\ &\quad -|i\rangle\langle j|l\rangle\langle l+1| - |i\rangle\langle j|l+1\rangle\langle l|) \\ &= V\sum_{i,j,l} c_i(t)c_j^*(t)(|l\rangle\langle j|\delta_{l+1,i} + |l+1\rangle\langle j|\delta_{l,i} - \\ &\quad -|i\rangle\langle l+1|\delta_{j,l} - |i\rangle\langle l|\delta_{j,l+1} \end{aligned} \tag{3.7}$$

More explicitly, the matrix elements $\rho_{m,n}$ are :

$$\begin{aligned} \rho_{m,n}(t) \equiv \langle m|\rho(t)|n\rangle &= \sum_{i,j} c_i(t)c_j^*(t)\langle m|i\rangle\langle j|n\rangle \\ &= \sum_{i,j} c_i(t)c_j^*(t)\delta_{m,i}\delta_{j,n} \quad \Rightarrow \\ \Rightarrow \rho_{m,n}(t) &= c_m(t)c_n^*(t) \end{aligned} \tag{3.8}$$

By this definition, we conclude to the Liouville-von Neumann equation :

$$
\begin{aligned}
i\frac{\partial}{\partial t}(\sum_{i,j} c_i(t)c_j^*(t)\langle m|i\rangle\langle j|n\rangle) &= V\sum_{i,j,l} c_i(t)c_j^*(t)(\langle m|l\rangle\langle j|n\rangle\delta_{l+1,i} + \langle m|l+1\rangle\langle j|n\rangle\delta_{l,i} - \\
&\quad -\langle m|i\rangle\langle l+1|n\rangle\delta_{j,l} - \langle m|i\rangle\langle l|n\rangle\delta_{j,l+1} \Rightarrow \\
\Rightarrow i\frac{\partial}{\partial t}\rho_{m,n}(t) &= V\sum_{i,j,l} c_i(t)c_j^*(t)(\delta_{m.l}\delta_{j,n}\delta_{l+1,i} + \delta_{m,l+1}\delta_{j,n}\delta_{l,i} - \\
&\quad -\delta_{m,i}\delta_{l+1,n}\delta_{j,l} - \delta_{m,i}\delta_{l,n}\delta_{j,l+1}) \\
\Rightarrow i\frac{\partial}{\partial t}\rho_{m,n}(t) &= V(\rho_{m+1,n}(t) + \rho_{m-1,n}(t) - \rho_{m,n+1}(t) - \rho_{m,n-1}(t) \quad (3.9)
\end{aligned}
$$

With the initial condition:

$$\rho_{m,n}(t=0) = c_m(t=0)c_{n=0}^*(t=0) = \delta_{m,0}\delta_{n,0} \tag{3.10}$$

In order to solve Eq. (3.9), as a first step we perform a discrete Fourier Transform over the site indices m and n, by multiplying each term by $e^{ikm}e^{-iqn}$ and summing over all m and n:

$$\rho^{k,q}(t) = \sum_{m,n} \rho_{m,n}(t)e^{i(km-qn)} \tag{3.11}$$

So, the produced momentum-space form of the LVN is:

$$
\begin{aligned}
i\sum_{m,n} \dot{\rho}_{m,n}(t)e^{ipm}e^{-iqn} &= V\sum_{m,n}(\rho_{m+1,n}(t) + \rho_{m-1,n}(t) - \rho_{m,n+1}(t) - \rho_{m,n-1}(t)) \\
&= V(e^{-ip}\sum_{m,n} \rho_{m+1,n}(t)e^{ipm}e^{-qn}e^{ip} + e^{ip}\sum_{m,n} \rho_{m-1,n}(t)e^{ipm}e^{-qn}e^{-ip} - \\
&\quad -e^{-iq}\sum_{m,n} \rho_{m,n-1}(t)e^{ipm}e^{-qn}e^{-iq} - e^{iq}\sum_{m,n} \rho_{m,n+1}(t)e^{ipm}e^{-qn}e^{iq}) \Rightarrow \\
\Rightarrow i\frac{\partial}{\partial t}\rho^{k,q}(t) &= V[(e^{ip} + e^{-ip}) - e^{iq} + e^{-iq})]\rho^{k,q}(t) \\
\Rightarrow i\frac{\partial}{\partial t}\rho^{k,q}(t) &= 2V[cos(k) - cos(q)]\rho^{k,q}(t) \quad (3.12)
\end{aligned}
$$

Solving Eq. 3.12 we get:

$$\rho^{k,q}(t) = \rho_0^{k,q}e^{-2iV[cos(k)-cos(q)]t} \tag{3.13}$$

Making use of the Jacobi−Anger expansion,

$$e^{\pm izcos(\phi)t} = \sum_n e^{\pm in\pi/2} e^{in\phi} J_n(z) \tag{3.14}$$

we express Eq. (3.13) in terms of ordinary Bessel functions J_n, and we arrive at the following form:

$$\rho^{k,q}(t) = \rho_0^{k,q} \sum_a e^{ia\pi/2} e^{iaq} J_a(2Vt) \sum_b e^{-ib\pi/2} e^{ibk} J_b(2Vt) \tag{3.15}$$

and we perform an inverse discrete Fourier Transformation, which yields the following expression for $\rho_{m,n}(t)$:

$$\begin{aligned} \rho_{m,n}(t) &= \sum_{k,q} e^{-ikm} e^{iqn} (\sum_{r,R} e^{ikr} e^{-iqR} \rho_{r,R}(0)) \\ &\quad \times \sum_{a,b} e^{ia\pi/2} e^{iaq} J_a(2Vt) e^{-ib\pi/2} e^{ibk} J_b(2Vt) \end{aligned} \tag{3.16}$$

We notice that:

$$\begin{aligned} \sum_k e^{-ikm} e^{ikr} e^{ibk} &= \delta_{m,b+r} \\ \sum_q e^{iqn} e^{-iqR} e^{iaq} &= \delta_{n,a-R} \end{aligned} \tag{3.17}$$

Therefore, the final form of the solution of the SLE, with the initial condition Eq. (3.10) is:

$$\begin{aligned} \rho_{m,n} &= \sum_{r,R} \sum_{a,b} \rho_{r,R}(0) e^{ia\pi/2} e^{-ib\pi/2} J_a(2Vt) J_b(2Vt) \delta_{m,b+r} \delta_{n,a-R} \\ &= \sum_{r,R} \rho_{r,R}(0) e^{i(n+R)\pi/2} e^{-i(m-r)\pi/2} J_{n+R}(2Vt) J_{m-r}(2Vt) \\ &= \sum_{r,R} \delta_{r,0} \delta_{R,0} e^{i(n+R)\pi/2} e^{-i(m-r)\pi/2} J_{n+R}(2Vt) J_{m-r}(2Vt) \\ &= e^{in\pi/2} e^{-im\pi/2} J_n(2Vt) J_m(2Vt) \\ &= i^{(n-m)} J_n(2Vt) J_m(2Vt) \end{aligned} \tag{3.18}$$

Where we have used the identity:

$$J_{-m}(z) = (-1)^m J_m(z) \tag{3.19}$$

We have all the tools we need to study the quantum motion of a charged particle on a discrete one-band lattice. For the case of vanishing electric field the exact value of $\langle l(t)\rangle$ and $\langle l^2(t)\rangle$, is found:

$$\langle l^2(t)\rangle = \sum_m m^2 \rho_{m,m} = \sum_m m^2 J_m^2(2Vt) = 2(Vt)^2 \tag{3.20}$$

To derive the above results we have used the following identity for the Bessel functions [12]:

$$\sum_m m^2 J_m^2(z) = z^2 \tag{3.21}$$

The MSD increases without bounds, since it is proportional to t^2. This is a known result, where an initially localized particle ($l = 0$), escapes to infinity, as a consequence of delocalization. We should note here, that the mean displacement for this simple case equals to zero. We expected this result, as it is a quantum motion in a closed system, and we need environmental coupling in order to produce a Quantum Ratchet.

3.2.2 Presence of Electric Field

By "turning on" the electric field [13] (Figure 3.2), an extra term is added to the Tight-Binding Hamiltonian which becomes:

$$H^0 = V \sum_l |l\rangle\langle l+1| + |l+1\rangle\langle l| + \mathscr{E}_0 f(t) \sum_l l|l\rangle\langle l| \tag{3.22}$$

where $\mathscr{E}_0$ and $f(t)$ is the amplitude and the time-dependence of the electric field respectively.

Again, by expressing the charged particle state $|\Psi(t)\rangle$ as linear combination of Wannier states (Eq. 3.4), we produce the Liouville-von Neumann in presence of time-dependent electric field :

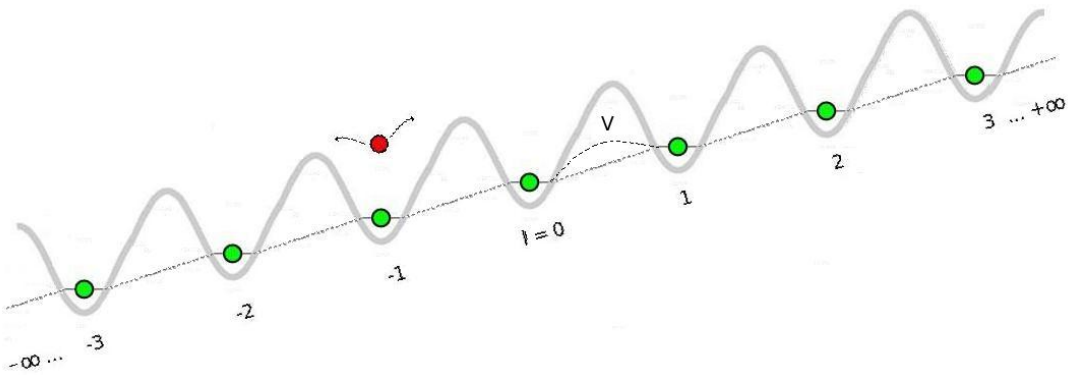

Figure 3.2: Quantum motion of a particle in 1-D discrete one-band lattice of l sites, under the presence of time-dependent (AC) electric field.

$$\begin{aligned} i\frac{\partial}{\partial t}\rho_{m,n}(t) &= V(\rho_{m+1,n}(t)+\rho_{m-1,n}(t)-\rho_{m,n+1}(t)-\rho_{m,n-1}(t))+ \\ &\quad +\mathscr{E}_0 f(t)(m-n)\rho_{m,n} \end{aligned} \tag{3.23}$$

In order to solve the above equation, we will use the transformation:

$$g_{m,n}(t) = \rho_{m,n}(t)e^{i\mathscr{E}_0(m-n)\eta(t)} \tag{3.24}$$

Where $\eta(t) = \int_0^t dt' f(t')$. Substituting the above in Eq. (3.23), we derive the time evolution equation for $g_{m,n}$:

$$i\frac{\partial}{\partial t}g_{m,n}(t) = V[(g_{m+1,n}(t)-g_{m,n-1}(t))_e^{-i\mathscr{E}_0\eta(t)} + (g_{m-1,n}(t)-g_{m,n+1}(t))e^{i\mathscr{E}_0\eta(t)}] \tag{3.25}$$

When we transform Eq. (3.25) into momentum-space, it takes the form:

$$i\frac{\partial}{\partial t}g^{k,q}(t) = 2V[cos(q-\mathscr{E}_0\eta(t))-cos(k-\mathscr{E}_0\eta(t))]g^{k,q} \tag{3.26}$$

Which is now easy to solve:

$$g^{k,q}(t) = g_0^{k,q}e^{-2iV\int_0^t dt'[cos(q-\mathscr{E}_0\eta(t'))-cos(k-\mathscr{E}_0\eta(t'))]g^{k,q}} \tag{3.27}$$

Using the definition of Eq. (3.24) in the transformation of Eq. (3.11) by adding, we obtain

$$\begin{aligned}\rho^{p,q}(t) &= \sum_{m,n}\rho_{m,n}(t)e^{i(pm-qn)} \\ &= \sum_{m,n}g_{m,n}e^{-i\mathscr{E}_0(m-n)\eta(t)}e^{i(pm-qn)} \\ &= \sum_{m,n}g_{m,n}e^{i([p-\mathscr{E}_0\eta(t)]m-[q-\mathscr{E}_0\eta(t)]n)} \\ &= g^{p-\mathscr{E}_0\eta(t),q-\mathscr{E}_0\eta(t)} \end{aligned} \tag{3.28}$$

So, the momentum-space form of the SLE is:

$$\rho^{p,q}(t)=\rho_0^{p-\mathscr{E}_0\eta(t),q-\mathscr{E}_0\eta(t)}e^{-2iV\int_0^t dt'[cos(q-\mathscr{E}_0\eta(t)-\mathscr{E}_0\eta(t'))-cos(p-\mathscr{E}_0\eta(t)-\mathscr{E}_0\eta(t'))]} \tag{3.29}$$

Following the same procedure, we use the Jacobi−Anger expansion for $e^{\pm izcos\phi}$ and for $e^{\pm izsin\phi}$:

$$\begin{aligned}e^{izsin\phi} &= \sum_n e^{in\phi}J_n(z) \\ e^{-izsin\phi} &= \sum_n(-1)^n e^{in\phi}J_n(z)\end{aligned} \tag{3.30}$$

We express Eq. (3.29) in terms of ordinary Bessel functions J_n and we get the following expression for $\rho^{k,q}(t)$:

$$\begin{aligned}\rho^{k,q}(t)=\rho_0^{k-\mathscr{E}_0\eta(t),q-\mathscr{E}_0\eta(t)}\sum_{a,b,c,d} & e^{-ia\pi/2}e^{iaq}J_a(2V\mathscr{U}(t))(-1)^bJ_b(2V\mathscr{V}(t)) \\ \times\quad & e^{ic\pi/2}e^{ick}J_c(2V\mathscr{U}(t))J_d(2V\mathscr{V}(t))e^{idk}\end{aligned} \tag{3.31}$$

Where

$$\mathscr{U}(t) = \int_0^t dt' Cos[\mathscr{E}_0(\eta(t)+\eta(t')] \tag{3.32}$$

$$\mathscr{V}(t) = \int_0^t dt' Sin[\mathscr{E}_0(\eta(t)+\eta(t')] \tag{3.33}$$

Performing an inverse discrete Fourier Transformation, we get:

$$\begin{aligned}\rho_{m,n}(t) &= \sum_{k,q} e^{-ikm}e^{iqn}(\sum_{r,R} e^{ikr}e^{-ik\mathscr{E}_0\eta(t)r}e^{-iqR}e^{iq\mathscr{E}_0\eta(t)R}\rho_{r,R}(0)) \sum_{a,b,c,d} e^{-ia\pi/2}e^{iaq}J_a(2V\mathscr{U}(t)) \\ &\times \quad (-1)^b J_b(2V\mathscr{V}(t))e^{ic\pi/2}e^{ick}J_c(2V\mathscr{U}(t))J_d(2V\mathscr{V}(t))e^{idk} \qquad (3.34)\end{aligned}$$

Again we notice that:

$$\begin{aligned}\sum_k e^{-ikm}e^{ikr}e^{ick}e^{idk} &= \delta_{m,r+c+d} \\ \sum_q e^{iqn}e^{-iqR}e^{iaq}e^{ibq} &= \delta_{n,R-a-b} \qquad (3.35)\end{aligned}$$

$$\begin{aligned}\Rightarrow \rho_{m,n}(t) &= \sum_{r,R}\sum_{a,b,c,d} e^{-ik\mathscr{E}_0\eta(t)r}e^{iq\mathscr{E}_0\eta(t)R}\rho_{r,R}(0)e^{-ia\pi/2}J_a(2V\mathscr{U}(t))J_{-b}(2V\mathscr{V}(t)) \\ &\times \quad e^{ic\pi/2}J_c(2V\mathscr{U}(t))J_d(2V\mathscr{V}(t))\delta_{m,r+c+d}\delta_{n,R-a-b} \\ &= \sum_{r,R}\sum_{a,c} e^{-ik\mathscr{E}_0\eta(t)r}e^{iq\mathscr{E}_0\eta(t)R}\rho_{r,R}(0)e^{-ia\pi/2}J_a(2V\mathscr{U}(t))J_{n+a-R}(2V\mathscr{V}(t)) \\ &\times \quad e^{ic\pi/2}J_c(2V\mathscr{U}(t))J_{m-r-c}(2V\mathscr{V}(t)) \qquad (3.36)\end{aligned}$$

Using Graf's addition theorem [14] for Bessel functions:

$$J_\nu(w)[Cos(\nu\chi), Sin(\nu\chi)] = \sum_k J_{\nu+k}(u)J_k(v)[Cos(k\alpha), Sin(k\alpha)] \qquad (3.37)$$

where,

$$\begin{aligned}w &= \sqrt{u^2+v^2-2uvCos\alpha} \\ u - vCos\alpha &= wCos\chi \\ vSin\alpha &= wSin\chi \qquad (3.38)\end{aligned}$$

$$
\begin{aligned}
\Rightarrow \rho_{m,n}(t) &= \sum_{r,R} e^{-ik\mathscr{E}_0\eta(t)r} e^{iq\mathscr{E}_0\eta(t)R} \rho_{r,R}(0) \sum_a J_a(2V\mathscr{U}(t)) J_{n+a-R}(2V\mathscr{V}(t)) [Cos(\alpha\frac{\pi}{2}) - iSin(\alpha\frac{\pi}{2})] \\
&\times \quad \sum_c J_c(2V\mathscr{U}(t)) J_{m-r-c}(2V\mathscr{V}(t)) [Cos(c\frac{\pi}{2}) + iSin(c\frac{\pi}{2})] \\
&= \sum_{r,R} e^{-ik\mathscr{E}_0\eta(t)r} e^{iq\mathscr{E}_0\eta(t)R} \rho_{r,R}(0) J_{n-R}(\mathscr{W}) [Cos[(n-R)Sin^{-1}(\frac{\mathscr{V}}{\mathscr{W}})] \\
&\qquad\qquad -iSin[(n-R)Sin^{-1}(\frac{\mathscr{V}}{\mathscr{W}}] \\
&\times \quad (-1)^{r-m} J_{r-m}(\mathscr{W}) \frac{1}{2} i [Sin[(r-m)Sin^{-1}(-\frac{\mathscr{V}}{\mathscr{W}})] - Sin[(r-m)Sin^{-1}(\frac{\mathscr{V}}{\mathscr{W}})] \\
&= \sum_{r,R} e^{-ik\mathscr{E}_0\eta(t)r} e^{iq\mathscr{E}_0\eta(t)R} \rho_{r,R}(0) J_{n-R}(\mathscr{W}) (-1)^{r-m} J_{r-m}(\mathscr{W}) (\frac{\mathscr{U} + i\mathscr{V}}{\mathscr{W}})^{R-n} (\frac{\mathscr{U} + i\mathscr{V}}{\mathscr{W}})^{m-r} \\
&= \sum_{r,R} e^{-ik\mathscr{E}_0\eta(t)r} e^{iq\mathscr{E}_0\eta(t)R} \rho_{r,R}(0) J_{n-R}(\mathscr{W}) J_{m-r}(\mathscr{W}) (\lambda)^{R-n} (\lambda)^{m-r} \\
&= \sum_{r,R} e^{-ik\mathscr{E}_0\eta(t)r} e^{iq\mathscr{E}_0\eta(t)R} \delta_{r,0}\delta_{R,0} J_{n-R}(\mathscr{W}) J_{m-r}(\mathscr{W}) (\lambda)^{R-n} (\lambda)^{m-r} \\
\Rightarrow \rho_{m,n}(t) &= \lambda^{m-n} J_m(\mathscr{W}) J_n(\mathscr{W})
\end{aligned}
\tag{3.39}
$$

The quantities $\mathscr{W}$ and λ, are given by

$$
\begin{aligned}
\mathscr{W} &= \sqrt{\mathscr{U}(t)^2 + \mathscr{V}(t)^2} \\
\lambda &= \sqrt{\frac{\mathscr{U}(t) + i\mathscr{V}(t)}{\mathscr{U}(t) - i\mathscr{V}(t)}}
\end{aligned}
\tag{3.40}
$$

We can further simplify Eq.(3.39) by noticing that $\mathscr{U}(t)^2 + \mathscr{V}(t)^2$ is exactly equal to $u(t)^2 + v(t)^2$, where

$$
\begin{aligned}
u(t) &= \int_0^t dt' Cos[\mathscr{E}_0\eta(t')] \\
v(t) &= \int_0^t dt' Sin[\mathscr{E}_0\eta(t')]
\end{aligned}
\tag{3.41}
$$

Now, we can compute the corresponding mean and mean square displacement:

$$\langle l(t)\rangle = \sum_m m\rho_{m,m} = \sum_m mJ_m^2(z) = 0 \tag{3.42}$$

$$\langle l^2(t)\rangle = \sum_m m^2\rho_{m,m} = \sum_m m^2 J_m^2(2V[u(t)^2 + v(t)^2]^{1/2}) = (2V)^2[u(t)^2 + v(t)^2] \tag{3.43}$$

For the special and very interesting case, of the sinusoidal field, i.e. $f(t) = Cos(\omega t)$, the quantities u and v are

$$u(t) = \frac{1}{\omega}\int_0^{\omega t} dt' Cos[(\mathscr{E}_0/\omega)sin(t')] \tag{3.44}$$

$$v(t) = \frac{1}{\omega}\int_0^{\omega t} dt' Sin[(\mathscr{E}_0/\omega)sin(t')] \tag{3.45}$$

We should notice here that the functions $u(t)$ and $v(t)$, whenever the upper limit ωt equals to $2\pi n$ (where n is an integer), are equal to $u(t) = J_0(\mathscr{E}_0/\omega)t$and $v(t) = 0$. So, these two functions for the special value $\omega t = 2\pi n$ are both bounded oscillatory functions of time. We will concentrate our interest for these special values. Therefore, the resulting forms for mean and mean squared displacement are:

$$\langle l(t)\rangle = 0 \tag{3.46}$$

$$\langle l^2(t)\rangle = 2V^2t^2J_0^2(\mathscr{E}_0/\omega) \tag{3.47}$$

We note here the well known phenomenon of dynamic localization that appears when the ratio $\mathscr{E}_0/\omega$ equals a root of J_0. In this case, the mean square displacement remains bounded, thus the moving particle remains localized under the action of a time-dependent electric field. This is illustrated in Figure 3.3 where we have plotted MSD as a function of time for the choice $\mathscr{E}_0/\omega$ equals the first root of J_0

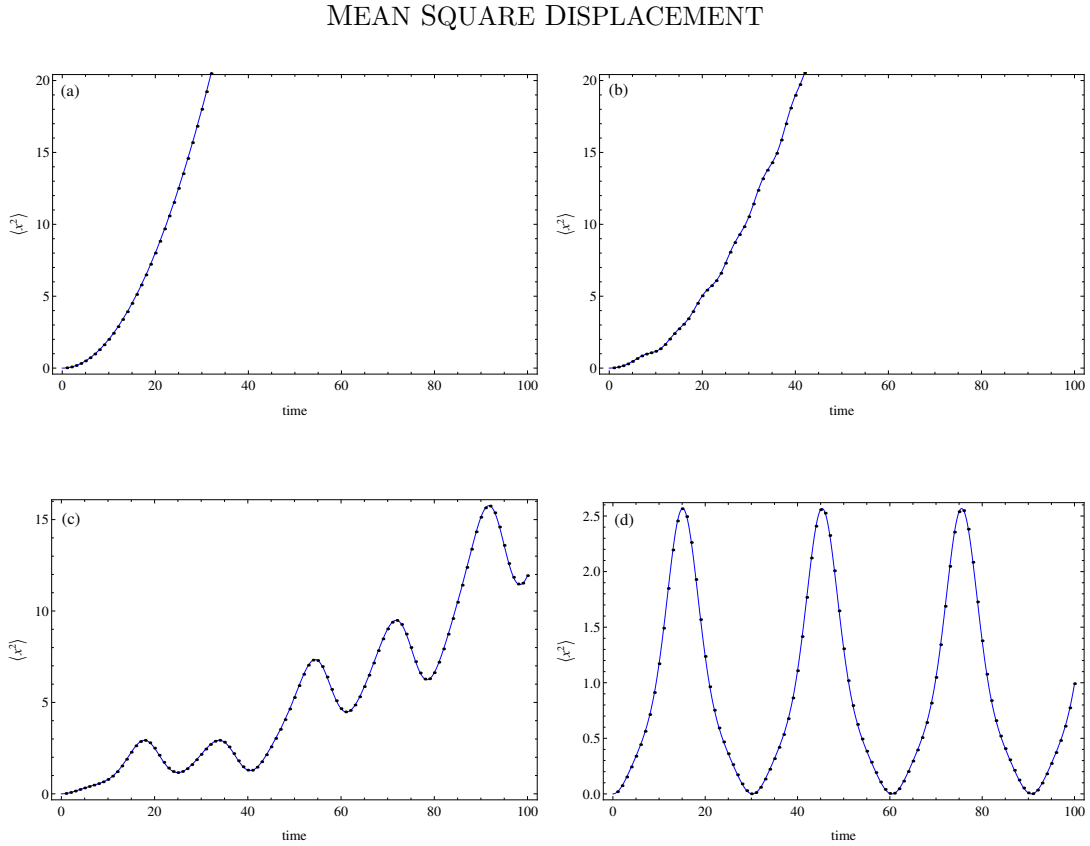

Figure 3.3: The mean square displacement, plotted as a function of time for different values of the ratio $\mathscr{E}_0/\omega$ for an AC field, whereas the ratio $\mathscr{E}_0/V$ is constant and equals 5. (a) $\mathscr{E}_0/\omega = 0$, (b) $\mathscr{E}_0/\omega = 1$, (c) $\mathscr{E}_0/\omega = 3$ and (d) $\mathscr{E}_0/\omega = 2.405$, which is the first root of $J_0(\mathscr{E}_0/\omega = 2.405)$ and shows the well known phenomenon of dynamic localization. The blue solid line corresponds to analytical solution, whereas the black dashed line corresponds to our numerical simulations.

3.3 1-D Discrete Two-Band Lattice

Let us continue with the case of quantum motion of a charged particle e, moving on a 1-D discrete two-band lattice [15–17], of sites l ($-\infty < l < \infty$), where the two bands of sites have an energy difference 2ϵ. We assume that, in the first band, all sites have constant on-site energy $-\epsilon$, while the second one, has sites with on-site energy equals to ϵ.

3.3.1 Absence of Electric Field

In this case, with the electric field set to zero, (Figure 3.4) the Tight−Binding Hamiltonian becomes:

$$H^0 = V\sum_l |l\rangle\langle l+1| + |l+1\rangle\langle l| + \epsilon\sum_l (-1)^l |l\rangle\langle l| \tag{3.48}$$

Where the extra term $\epsilon\sum_l (-1)^l |l\rangle\langle l|$ denotes each site's (constant) on-site energy.

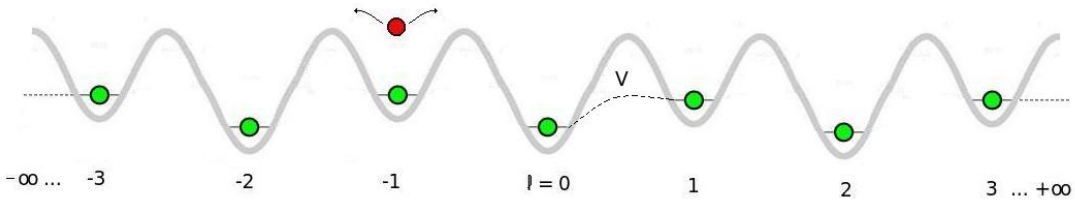

Figure 3.4: Quantum motion of a particle in 1-D discrete two-band lattice of l sites, in the absence of electric field. The two bands, have an energy difference 2ϵ.

As in the previous section the LVN, has the following form:

$$i\frac{\partial}{\partial t}\rho_{m,n} = V(\rho_{m+1,n} + \rho_{m-1,n} - \rho_{m,n+1} - \rho_{m,n-1}) + \epsilon[(-1)^m - (-1)^n]\rho_{m,n} \tag{3.49}$$

Unfortunately, Eq. (3.49) has no analytical solution for this case. Therefore, we will study the quantum motion in 1-D discrete two-band lattice numerically. We will provide numerical results of the solution of Eq.(3.49) where we used a lattice, of 150 sites (75 sites per band), that is a fair approximation of the infinite lattice. Moreover, we set the nearest-neighbor intersite interactions V to 0.1 and on-sites' energy ϵ to 0.1. In Figure 3.5 we can see, again that an initially localized particle (at site l = 0), delocalized through time, and escapes to infinity, since the MSD $\propto t^2$. The difference with the MSD in 1-D discrete one-band lattice is the factor, which multiplies the term t^2. From best fit to our data we find that this factor has the value 0.0035 in contrast with the previous section, where that factor had the value 0.02. As we can see, the energy difference between the sites decreases the diffusion.

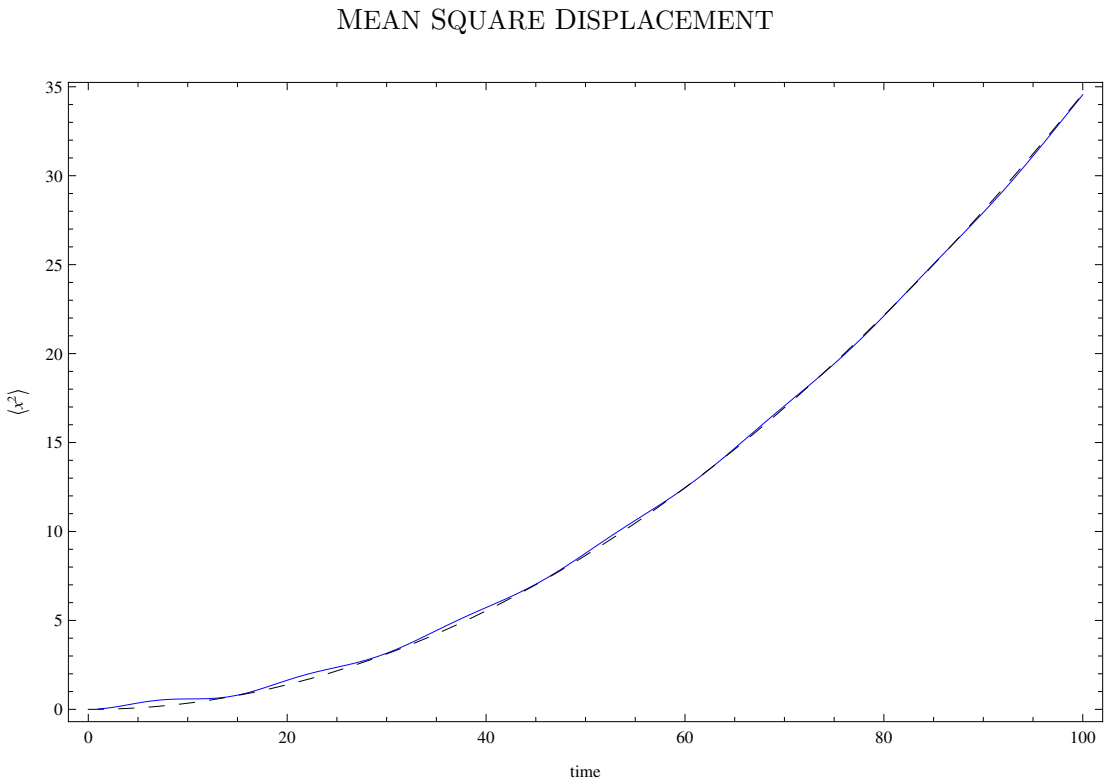

Figure 3.5: The numerical simulation of mean square displacement, plotted as a function of time for the 1-D discrete two-band lattice. The blue solid line corresponds to our numerical results and the black dashed line corresponds to best fit of our data.

3.3.2 Presence of Electric Field

Continuing with the same procedure, we will add a time-dependent electric field (Figure 3.6). As a result, the Tight-Binding Hamiltonian is

$$\begin{aligned} H^0 &= V\sum_l |l\rangle\langle l+1| + |l+1\rangle\langle l| + \epsilon\sum_l (-1)^l |l\rangle\langle l| + \\ &\quad + \mathscr{E}_0 f(t)\sum_l l|l\rangle\langle l| \end{aligned} \tag{3.50}$$

The LVN for this case, now becomes :

$$\begin{aligned} i\frac{\partial}{\partial t}\rho_{m,n} &= V(\rho_{m+1,n} + \rho_{m-1,n} - \rho_{m,n+1} - \rho_{m,n-1}) + \epsilon[(-1)^m - (-1)^n]\rho_{m,n} + \\ &\quad + \mathscr{E}_0 f(t)(m-n)\rho_{m,n} \end{aligned} \tag{3.51}$$

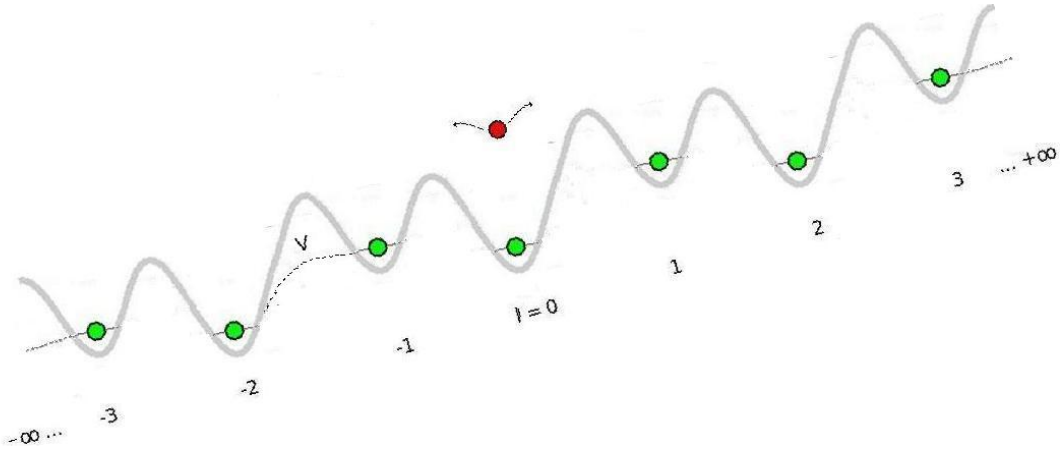

Figure 3.6: Quantum motion of a particle in 1-D discrete two-band lattice of l sites, in the presence of time-dependent (AC) electric field.

As in the previous subsection, there is no analytical solution for this LVN equation. Therefore, we will study the quantum motion in 1-D discrete two-band lattice in presence of electric field numerically. The two-band lattice, consisted the same number of sites, i.e 150. Furthermore, the nearest-neighbor intersite interactions V and the on-sites' energy ϵ have the same values as before. We evaluate the MSD as a function of time, for different values of the ratio $\mathscr{E}_0/\omega$ for the case of a sinusoidal electric field ($f(t) = cos(\omega t)$), as the ratio $\mathscr{E}_0/V$ was kept constant equal to 5. From the graph that follows below, one can discern that the phenomenon of dynamic localization, that was present in the discrete one-band lattice for the special case $\mathscr{E}_0/\omega$ equals to a root of J_0, now disappears. The initially localized particle diffuses through time and the MSD remains unbounded.

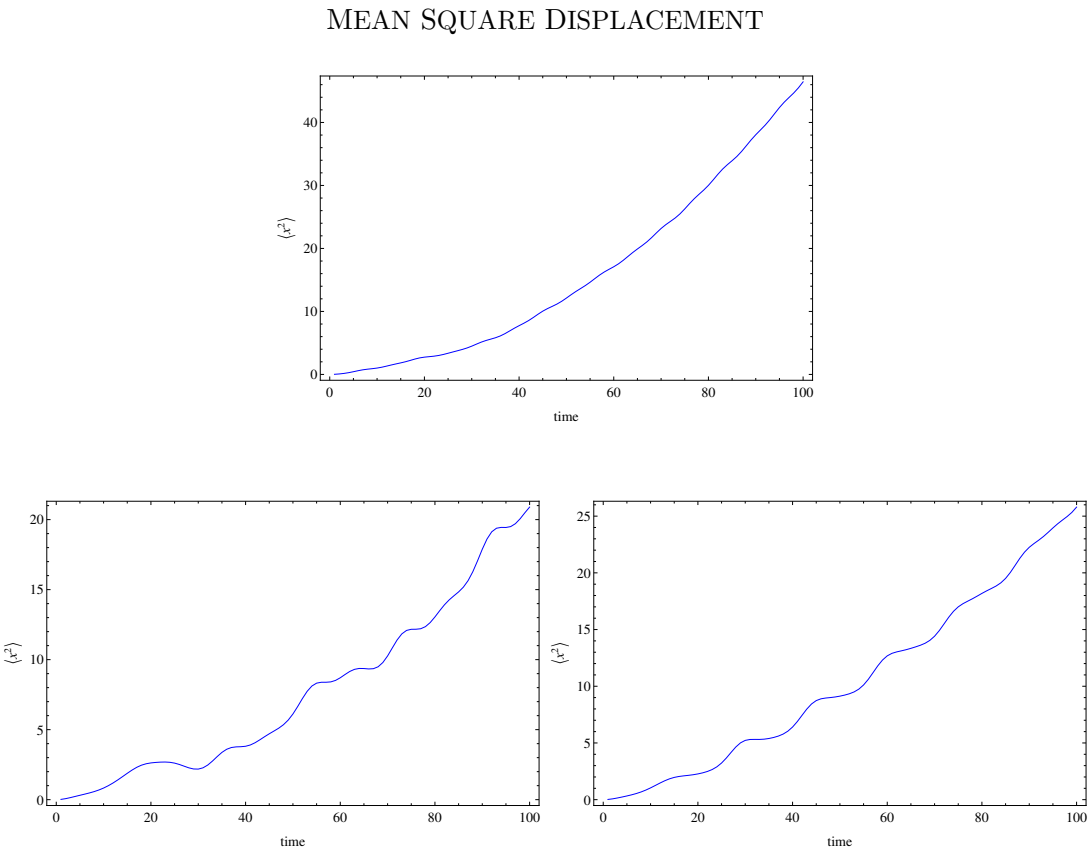

Figure 3.7: The numerical simulation of mean square displacement, plotted as a function of time for the 1-D discrete two-band lattice in presence of a sinusoidal electric field, for different values of the ratio $\mathscr{E}_0/\omega$. The ratio $\mathscr{E}_0/V$ is constant and equals 5. (a) $\mathscr{E}_0/\omega = 1$, (b) $\mathscr{E}_0/\omega = 3$, (c) $\mathscr{E}_0/\omega = 2.405$. We notice here, the disappearance of the dynamic localization phenomenon, for the value $\mathscr{E}_0/\omega = 2.405$.

3.4 1-D Discrete Three-Band Lattice

The final case of our interest for the quantum motion of a charged particle e, is on a 1-D discrete three-band lattice, of sites l ($-\infty < l < \infty$). Now, our lattice consisted by three bands of sites, each doublet of them has a minimum energy difference 2ϵ and maximum of 4ϵ. We assume that, in the first band, all sites have constant on-site energy $-\epsilon$, while the second one, has sites with on-site energy equals to ϵ and the third one has sites with on-site energy equals to 3ϵ.

3.4.1 Absence of Electric Field

In the absence of the electric field (Figure 3.8), we will use another way to introduce the Tight−Binding Hamiltonian for this case:

$$H^0 = V \sum_l |l\rangle\langle l+1| + |l+1\rangle\langle l| + \sum_l \epsilon_l |l\rangle\langle l| \tag{3.52}$$

Where now the term $\sum_l \epsilon_l |l\rangle\langle l|$ denotes each site's constant on-site energy, for the three bands $(l, l+1, L+2)$

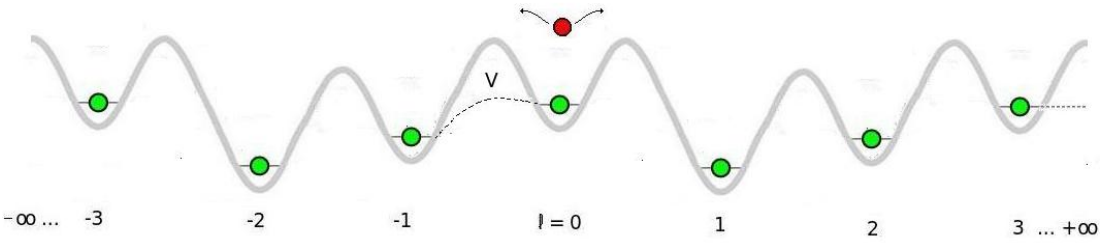

Figure 3.8: Quantum motion of a particle in 1-D discrete three-band lattice of l sites, in the absence of electric field. The three bands, have a minimum energy difference 2ϵ and a maximum 4ϵ. The index l denotes the first band, $l+1$ the second an $l+2$ the third one.

The following equation represents the LVN equation for a quantum motion of a charged particle in a discrete three-band lattice :

$$i\frac{\partial}{\partial t}\rho_{m,n} = V(\rho_{m+1,n} + \rho_{m-1,n} - \rho_{m,n+1} - \rho_{m,n-1}) + [\epsilon_m - \epsilon_n]\rho_{m,n} \tag{3.53}$$

There is no analytical solution for this case too, therefore, we will continue by examining this quantum motion numerically. We used a lattice, consisted of 150 sites (50 sites per band). Moreover, we set the nearest-neighbor intersite interactions V to 0.1 and on-sites' energy ϵ to 0.1. The next Figure (4.4) of MSD as a function of time, show us the expected result of the delocalization of the initially localized particle. From best fit to our data we can see that the diffusion in three-band lattice decreases in contrast with the previous lattices, since the factor which multiplies the term t^2 is 0.0014.

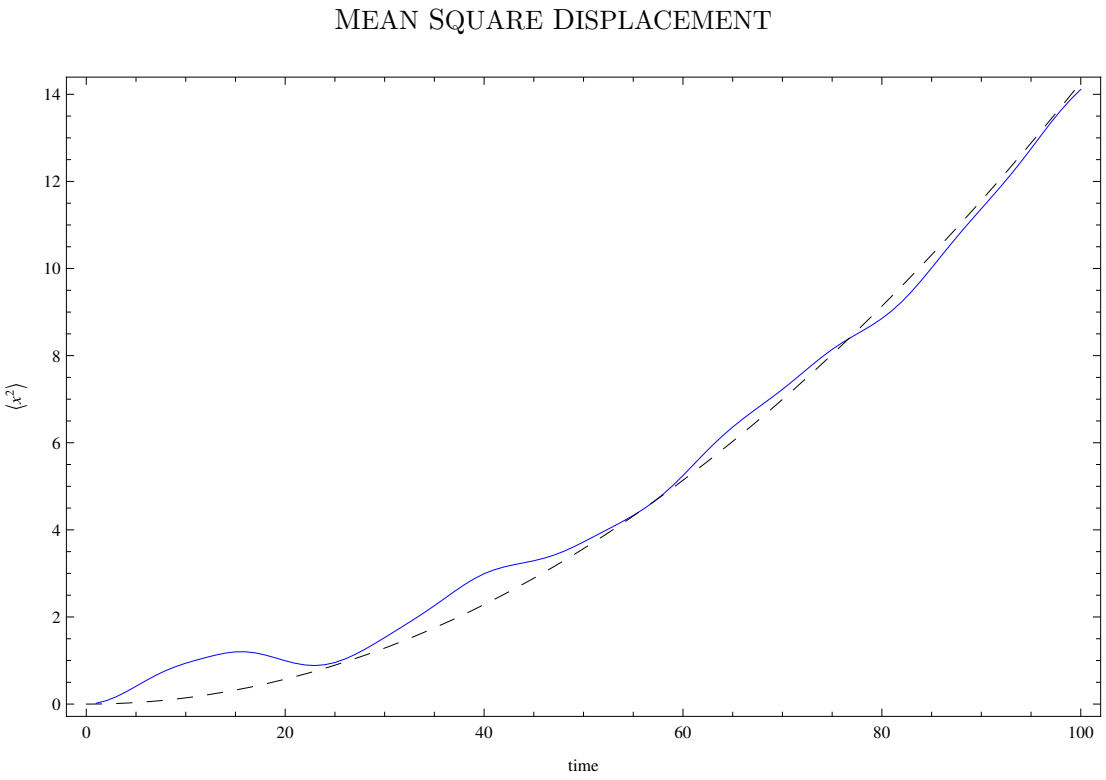

Figure 3.9: The numerical simulation of mean square displacement, plotted as a function of time for the 1-D discrete three-band lattice. The blue solid line corresponds to our numerical results and the black dashed line corresponds to best fit of our data.

3.4.2 Presence of Electric Field

Adding a time-dependent electric field (Figure 3.10), the new Tight-Binding Hamiltonian is

$$\begin{aligned} H^0 &= V\sum_l |l\rangle\langle l+1| + |l+1\rangle\langle l| + \sum_l \epsilon_l |l\rangle\langle l| + \\ &\quad + \mathscr{E}_0 f(t) \sum_l l|l\rangle\langle l| \end{aligned} \tag{3.54}$$

The LVN equation under the presence of an AC electric field becomes :

$$\begin{aligned} i\frac{\partial}{\partial t}\rho_{m,n} &= V(\rho_{m+1,n} + \rho_{m-1,n} - \rho_{m,n+1} - \rho_{m,n-1}) + [\epsilon_m - \epsilon_n]\rho_{m,n} + \\ &\quad + \mathscr{E}_0 f(t)(m-n)\rho_{m,n} \end{aligned} \tag{3.55}$$

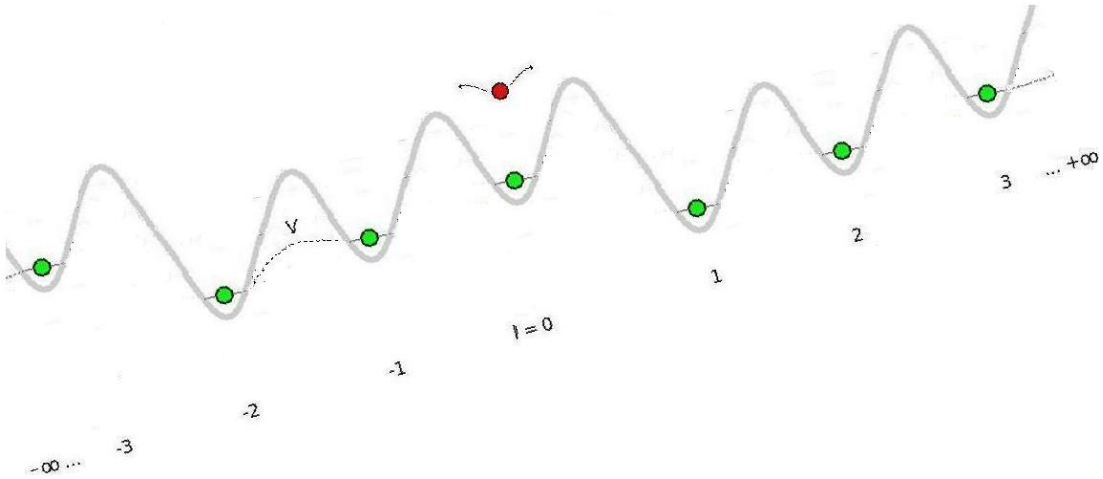

Figure 3.10: Quantum motion of a particle in 1-D discrete three-band lattice of l sites, in the presence of time-dependent (AC) electric field.

The numerical solution of the LVN equation (Eq.3.55), for the quantum motion in 1-D discrete three-band lattice in the presence of electric field, follows by providing the MSD as a function of time (Figure 4.5), for different values of the ratio $\mathscr{E}_0/\omega$, as we have done in previous sections . Again we choose the case of a sinusoidal electric field ($f(t) = cos(\omega t)$) and the ratio $\mathscr{E}_0/V$ was kept constant equal to 5. The three-band lattice, is consisted of the same number of sites and the nearest-neighbor intersite interactions V and the on-sites' energy ϵ have the same values as before. The discrete three-band lattice, appears to have the same behavior, i.e. the initially localized particle diffuses through time, and the MSD remains unbounded for each value of the ratio $\mathscr{E}_0/\omega$.

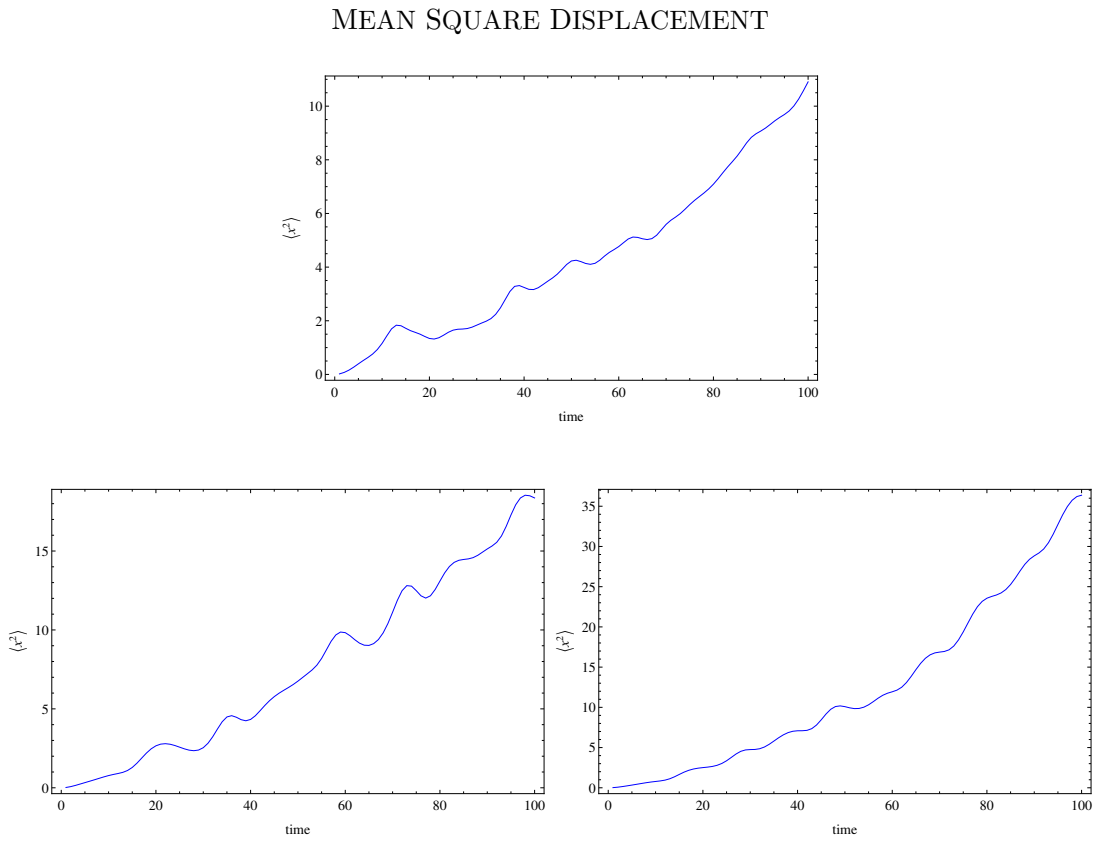

Figure 3.11: The numerical simulation of mean square displacement, plotted as a function of time for the 1-D discrete three-band lattice in presence of a sinusoidal electric field, for different values of the ratio $\mathscr{E}_0/\omega$. The ratio $\mathscr{E}_0/V$ is constant and equals 5. (a) $\mathscr{E}_0/\omega = 1$, (b) $\mathscr{E}_0/\omega = 3$, (c) $\mathscr{E}_0/\omega = 2.405$. The phenomenon of dynamic localization does not appear for these parameter values.

4 Quantum Motion In an Open System

4.1 Introduction

The theory and the analysis of the one dimensional motion of a charged particle, on three separate lattices in the presence/absence of a time-dependent electric field (sinusoidal), was developed in Chapter 3. Now, we will consider the quantum motion of a charged particle in an open system. We introduce the effect of dynamical disorder, through a set of hermitian Lindblad operators [18]:

$$L_l = \frac{\sqrt{\alpha}}{2}|l\rangle\langle l| \tag{4.1}$$

that project on to the lattice sites' orbitals as explained in Chapter 1. The Lindblad operators satisfy the coupling of the charged particle with the environment (e.g. the thermal phonons). In the following sections, we study this quantum motion, using the same sequence as in Chapter 3. First, we examine the simplest case of the quantum motion in a discrete one-band lattice , and we obtain exact solutions for the mean square displacement (**MSD**), by solving the stochastic Liouville equation (**SLE**), which now

has the form:

$$i\frac{\partial}{\partial t}\rho_{m,n} = V(\rho_{m+1,n}+\rho_{m-1,n}-\rho_{m,n+1}-\rho_{m,n-1})+\mathscr{E}_0 f(t)(m-n)\rho_{m,n} \\ -i\alpha(1-\delta_{m,n})\rho_{m,n} \tag{4.2}$$

for various values of $\mathscr{E}_0$ (including the trivial case, when $\mathscr{E}_0 = 0$). Again, since we have an analytical form of the MSD, we will compare it with our numerical results. In the next section, we present our numerical simulations for the MSD as a function of time, for the quantum motion in a two-band lattice, where as usual, each band has different energy. This is expressed by the following SLE:

$$i\frac{\partial}{\partial t}\rho_{m,n} = V(\rho_{m+1,n}+\rho_{m-1,n}-\rho_{m,n+1}-\rho_{m,n-1})+\mathscr{E}_0 f(t)(m-n)\rho_{m,n} \\ +\epsilon[(-1)^m-(-1)^n]\rho_{m,n}-i\alpha(1-\delta_{m,n})\rho_{m,n} \tag{4.3}$$

In the last section, we consider a discrete three-band lattice. The equation, which describes such a quantum motion is :

$$i\frac{\partial}{\partial t}\rho_{m,n} = V(\rho_{m+1,n}+\rho_{m-1,n}-\rho_{m,n+1}-\rho_{m,n-1})+\mathscr{E}_0 f(t)(m-n)\rho_{m,n} \\ +[\epsilon_m-\epsilon_n]\rho_{m,n}-i\alpha(1-\delta_{m,n})\rho_{m,n} \tag{4.4}$$

4.2 1-D Discrete One-Band Lattice

We begin with the quantum motion of a charged particle e, moving on dynamically disorder 1-D discrete one-band lattice of sites l (-∞ < l < ∞), in the absence of on-site energy. Here, the disorder involved is introduced through a set of Lindblad operators that project onto the lattice sites, which represent the environmental coupling with the charged particle.

4.2.1 Absence of Electric Field

In the case of a zero electric field, the Tight-Binding Hamiltonian has the well known form :

$$H^0 = V\sum_l |l\rangle\langle l+1| + |l+1\rangle\langle l| \tag{4.5}$$

where V is the nearest-neighbor intersite interactions (overlap integrals), and the sum is over the N lattice sites , where $|l\rangle$ represents a Wannier state localized on lattice site l.

The evolution equation for the reduced density matrix for the particle, given by the Liouville-Von Neumann equation is

$$i\frac{\partial}{\partial t}\rho(t) = [H^0, \rho(t)] - \sum_l [L_l, [L_l, \rho]] \qquad (\hbar = 1) \tag{4.6}$$

Where, the first order at the RHS gives the unitary evolution, while the second term gives the non-unitary (incoherent) evolution causing the initially pure density matrix ($t = 0$) to become mixed ($t > 0$). In terms of its matrix elements $\rho_{m,n}$, one obtains the form of the SLE [19]:

$$\begin{aligned} i\frac{\partial}{\partial t}\rho_{m,n} &= V(\rho_{m+1,n} + \rho_{m-1,n} - \rho_{m,n+1} - \rho_{m,n-1}) - \\ &\quad -i\alpha(1 - \delta_{m,n})\rho_{m,n} \end{aligned} \tag{4.7}$$

In attempting to solve Eq. (4.7) for $\rho_{m,n}(t)$, we use the analogous method as in Chapter 3. We perform a discrete Fourier Transform over the site labels m and n (Eq. 3.13), by multiplying each term by $e^{ikm}e^{-iqn}$ and summing over all m and n. The produced momentum-space form of the SLE :

$$\begin{aligned} i\frac{\partial}{\partial t}\rho^{k,q} &= 2V[cos(k) - cos(q)]\rho^{k,q} - i\alpha\rho^{k,q} \\ &\quad +i\alpha\sum_m \rho_{m,m}e^{i(k-q)m} \end{aligned} \tag{4.8}$$

Using the integrating factor method, we arrive at:

$$\begin{aligned} \rho^{k,q}(t) &= \rho_0^{k,q}e^{2iV[cos(k)-cos(q)]t}e^{-\alpha t} + \alpha\int_0^t dt' \sum_m e^{-i(k-q)m}\rho_{m,m}(t') \\ &\times \quad e^{2iV[cos(k)-cos(q)](t-t')}e^{-\alpha(t-t')} \end{aligned} \tag{4.9}$$

Setting $k = k'$ and $q = k' - k$ in Eq. (4.9) and summing over all k', we obtain the evolution of a new quantity $P^k(t)$, defined by:

$$\begin{aligned} P^k(t) &= \sum_{k'} \rho^{k',k'-k}(t) = \sum_{k'} (\sum_{m,n} \rho_{m,n} e^{ik'm} e^{-ik'n} e^{ikn}) \\ &= \sum_{m,n} \rho_{m,n} e^{ikn} (\sum_{k'} e^{ik'm} e^{-ik'n}) = \sum_{m,n} \rho_{m,n} e^{ikn} \delta_{m,n} \\ &= \sum_{m} \rho_{m,m} e^{ikm} \end{aligned} \tag{4.10}$$

By substituting this transformation in Eq. (4.9), one obtains :

$$\begin{aligned} P^k(t) &= \sum_{k'} \rho_0^{k',k'-k} e^{2iv[cos(k')-cos(k'-k)]t} e^{-at} \\ &\quad + \alpha \int_0^t dt' e^{-\alpha(t-t')} \sum_{k'} (\sum_{m} e^{ikm} \rho_{m,m}(t')) e^{2iv[cos(k')-cos(k'-k)](t-t')} \\ &= \sum_{k'} \rho_0^{k',k'-k} e^{2iv[cos(k')-cos(k'-k)]t} e^{-at} + \alpha \int_0^t dt' e^{-\alpha(t-t')} P^k(t') \\ &\quad \times \sum_{k'} e^{2iv[cos(k')-cos(k'-k)](t-t')} \end{aligned} \tag{4.11}$$

By the definition of P^k,Eq. (4.10), one can easily extract exactly the mean square displacement, as follows:

$$\langle l^2 \rangle(t) = -\frac{\partial^2}{\partial k^2} P^k \Big|_{k=0} \tag{4.12}$$

Used in conjunction with Eq. (4.11), gives :

$$\begin{aligned} \langle l^2 \rangle(t) &= e^{-\alpha t} \sum_{k'} -\frac{\partial^2}{\partial k^2} \rho_0^{k',k'-k} e^{2iv[cos(k')-cos(k'-k)]t} \Big|_{k=0} \\ &\quad + \alpha \int_0^t dt' e^{-\alpha(t-t')} \left. -\frac{\partial^2}{\partial k^2} P^k(t') \right|_{k=0} \sum_{k'} e^{2iv[cos(k')-cos(k'-k)](t-t')} \\ &\quad + \alpha \int_0^t dt' e^{-\alpha(t-t')} P^k(t') \sum_{k'} -\frac{\partial^2}{\partial k^2} e^{2iv[cos(k')-cos(k'-k)](t-t')} \Big|_{k=0} \end{aligned} \tag{4.13}$$

Simplifying Eq. (4.13), we introduce two new quantities :

$$\theta_k''(t) = \sum_{k'} -\frac{\partial^2}{\partial k^2}\rho_0^{k',k'-k} e^{2iv[cos(k')-cos(k'-k)]t}\Big|_{k=0} \tag{4.14}$$

$$\begin{aligned}
\psi_k''(t,t') &= -\frac{\partial^2}{\partial k^2}\sum_{k'} e^{2iv[cos(k')-cos(k'-k)](t-t')}\Big|_{k=0} \\
&= -\frac{\partial^2}{\partial k^2}\sum_{k'}\sum_{m} e^{im\frac{\pi}{2}} e^{imk'} J_m(2V(t-t')) \\
&\quad \times \sum_{n} e^{-in\frac{\pi}{2}} e^{ink'} e^{-ink} J_n(2V(t-t'))\Big|_{k=0} \\
&= -\frac{\partial^2}{\partial k^2}\sum_{m} e^{im\pi} e^{imk} J_{-m}(2V(t-t'))J_m(2V(t-t'))\Big|_{k=0} \\
&= -\frac{\partial^2}{\partial k^2} e^{imk} J_m^2(2V(t-t'))\Big|_{k=0} \\
&= -\frac{\partial^2}{\partial k^2} J_0(4V(t-t'))sin(\frac{k}{2})\Big|_{k=0} \\
&= \frac{[4V(t-t')]^2}{8} = 2V^2(t-t')^2
\end{aligned} \tag{4.15}$$

Where in the last equation for $\psi_k''(t,t')$, we have used some identities for the Bessel functions (Eq.(3.30)). Differentiating Eq. (4.13) with respect to time, gives :

$$\begin{aligned}
\frac{d}{dt}\langle l^2\rangle(t) &= -\alpha e^{-\alpha t}\theta_k''(t) + e^{-\alpha t}\frac{d}{dt}\theta_k''(t) + \alpha(\langle l^2\rangle(t) \\
&\quad -\alpha\int_0^t dt' e^{-\alpha(t-t')}\langle l^2\rangle(t')) + \alpha(\psi_k''(t,t) - \alpha\int_0^t dt' e^{-\alpha(t-t')}\psi_k''(t,t') \\
&\quad + \int_0^t dt' e^{-\alpha(t-t')}\frac{d}{dt}\psi_k''(t,t')) \\
\Rightarrow \frac{d}{dt}\langle l^2\rangle(t) &= e^{-\alpha t}\frac{d}{dt}\theta_k''(t) + \alpha\int_0^t dt' e^{-\alpha(t-t')}\frac{d}{dt}\psi_k''(t,t')
\end{aligned} \tag{4.16}$$

Substituting Eq. (4.15) in Eq.(4.16) we get:

$$\begin{aligned}
\frac{d}{dt}\langle l^2\rangle(t) &= e^{-\alpha t}\frac{d}{dt}\theta_k''(t) + \alpha\int_0^t dt' e^{-\alpha(t-t')}4V^2(t-t') \\
&= e^{-\alpha t}\frac{d}{dt}\theta_k''(t)\frac{4V^2 e^{-\alpha t}(-\alpha t + e^{\alpha t} - 1)}{\alpha} \\
&= e^{-\alpha t}\frac{d}{dt}[\theta_k''(t) - \psi_k''(t,0)] + \frac{4V^2}{\alpha} - \frac{4V^2}{\alpha}e^{-\alpha t}
\end{aligned} \tag{4.17}$$

If the initial density matrix is site diagonal, $\theta''_k(t) = \psi''_k(t,0)$ and Eq. (4.17) becomes, for long time :

$$\langle l^2\rangle(t) - \langle l^2\rangle(0) = \frac{4V^2}{\alpha}t \tag{4.18}$$

As one can see the MSD increases linear with time ($\propto t$). That means, the initially localized particle ($l = 0$) coupled with the environment, finally diffuses through the lattice and escapes to infinity.

4.2.2 Presence of Electric Field

We continue with the Tight-Binding Hamiltonian for the charged particle, on the discrete one-band lattice, in the presence of arbitrary (for now) Electric Field, which has the form :

$$H^0 = V\sum_l |l\rangle\langle l+1| + |l+1\rangle\langle l| + \mathscr{E}_0 f(t)\sum_l l|l\rangle\langle l| \tag{4.19}$$

where $\mathscr{E}_0$ and $f(t)$, is the amplitude and the time-dependence of the electric field respectively. Using again the Liouville-Von Neumann equation (Eq. 4.6) in terms of its matrix elements $\rho_{m,n}$, we get the following form of the SLE [19]:

$$\begin{aligned} i\frac{\partial}{\partial t}\rho_{m,n}(t) &= V(\rho_{m+1,n}(t) + \rho_{m-1,n}(t) - \rho_{m,n+1}(t) - \rho_{m,n-1}(t)) + \\ &\quad +\mathscr{E}_0 f(t)(m-n)\rho_{m,n} - i\alpha(1-\delta_{m,n})\rho_{m,n} \end{aligned} \tag{4.20}$$

Performing, as usual, a discrete Fourier Transform over the site labels m and n (Eq. 3.13), we produce the momentum-space form of the SLE, which now becomes :

$$\begin{aligned} \rho^{k,q}(t) &= i(t)\mathscr{E}_0 f(t)(\frac{\partial}{\partial k} + \frac{\partial}{\partial q})\rho^{k,q} + 2V[cos(k) - cos(q)]\rho^{k,q} - i\alpha\rho^{k,q} \\ &\quad +i\alpha\sum_m \rho_{m,m}e^{i(k-q)m} \end{aligned} \tag{4.21}$$

In order to solve the above equation, we will make a step back and according to transformation eq. (3.24), we transform Eq. (4.20) in a time evolution equation for $g_{m,n}$, and we perform a discrete Fourier Transform in the new one. Finally, we conclude :

$$
\begin{aligned}
i\frac{\partial}{\partial t}g^{k,q}(t) &= 2V[cos(q-\mathscr{E}_0\eta(t))-cos(k-\mathscr{E}_0\eta(t))]g^{k,q} \\
&\quad -i\alpha g^{k,q}+i\alpha\sum_m g_{m,m}e^{i(k-q)m}
\end{aligned}
\tag{4.22}
$$

Where $\eta(t) = \int_0^t dt' f(t')$. Now it is easy to solve, according to integrating factor method, and make an inverse transformation of Eq. (3.24), aiming the final solution of Eq. (4.21),i.e.

$$
\begin{aligned}
\rho^{k,q}(t) &= \rho_0^{k-\mathscr{E}_0\eta(t),q-\mathscr{E}_0\eta(t)}e^{2iV\int_0^t dt'[cos(k-\mathscr{E}_0\eta(t)-\mathscr{E}_0\eta(t'))-cos(q-\mathscr{E}_0\eta(t)-\mathscr{E}_0\eta(t'))]}e^{-\alpha t} \\
&\quad +\alpha\int_0^t dt'\sum_m e^{-i(k-q)m}\rho_{m,m}(t')e^{2iV\int_{t'}^t dt''[cos(k-\mathscr{E}_0\eta(t)-\mathscr{E}_0\eta(t''))-cos(q-\mathscr{E}_0\eta(t)-\mathscr{E}_0\eta(t''))]} \\
&\quad \times\ e^{-\alpha(t-t')}
\end{aligned}
\tag{4.23}
$$

Setting again $k = k'$ and $q = k' - k$ in the above equation, we obtain the equation of evolution of the quantity $P^k(t)$, for this case, which is:

$$
\begin{aligned}
P^k(t) &= \sum_{k'}\rho_0^{k'-\mathscr{E}_0\eta(t),k'-k-\mathscr{E}_0\eta(t)}e^{2iV\int_0^t dt'[cos(k'-\mathscr{E}_0\eta(t)-\mathscr{E}_0\eta(t'))-cos(k'-k-\mathscr{E}_0\eta(t)-\mathscr{E}_0\eta(t'))]}e^{-\alpha t} \\
&\quad +\alpha\int_0^t dt' P^k(t')\sum_{k'} e^{2iV\int_{t'}^t dt''[cos(k-\mathscr{E}_0\eta(t)-\mathscr{E}_0\eta(t''))-cos(q-\mathscr{E}_0\eta(t)-\mathscr{E}_0\eta(t''))]} \\
&\quad \times\ e^{-\alpha(t-t')}
\end{aligned}
\tag{4.24}
$$

The definition of mean square displacement, Eq. (4.12), and a derivation with respect to time, gives :

$$
\frac{d}{dt}\langle l^2\rangle(t) = e^{-\alpha t}\frac{d}{dt}\theta_k''(t)+\alpha\int_0^t dt' e^{-\alpha(t-t')}\frac{d}{dt}\psi_k''(t,t') \tag{4.25}
$$

Where now $\theta_k''(t)$ and $\psi_k''(t,t')$, have the following form:

$$\theta''_k(t) = \sum_{k'} -\frac{\partial^2}{\partial k^2}\rho_0^{k'-\mathscr{E}_0\eta(t),k'-k-\mathscr{E}_0\eta(t)} \times e^{2iv\int_0^t dt'[cos(k'-\mathscr{E}_0\eta(t)-\mathscr{E}_0\eta(t'))-cos(k'-k-\mathscr{E}_0\eta(t)-\mathscr{E}_0\eta(t'))]}\Big|_{k=0} \quad (4.26)$$

$$\begin{aligned}\psi''_k(t,t') &= -\frac{\partial^2}{\partial k^2}e^{2iv\int_{t'}^t dt''[cos(k'-\mathscr{E}_0\eta(t)-\mathscr{E}_0\eta(t''))-cos(k'-k-\mathscr{E}_0\eta(t)-\mathscr{E}_0\eta(t''))]}\Big|_{k=0} \\ &= -\frac{\partial^2}{\partial k^2}\sum_m e^{ikm}J_m^2(2[u^2(t,t')+v^2(t,t')]^{1/2})\Big|_{k=0} \\ &= -\frac{\partial^2}{\partial k^2}J_0(4[u^2(t,t')+v^2(t,t')]^{1/2}sin(\frac{k}{2})\Big|_{k=0} \\ &= 2V^2[u^2(t,t')+v^2(t,t')] \quad (4.27)\end{aligned}$$

For the last equation, we use the identities for Bessel functions, the Graf's Theorem, as also the trigonometric property $\mathscr{U}^2(t,t')+\mathscr{V}^2(t,t')=u^2(t,t')+v^2(t,t')$, described in the previous Chapter. The quantities $u(t,t')$ and $v(t,t')$, were defined as

$$\begin{aligned}u(t,t') &= \int_{t'}^t dt'' Cos[\mathscr{E}_0\eta(t'')] \\ v(t,t') &= \int_{t'}^t dt'' Sin[\mathscr{E}_0\eta(t'')] \quad (4.28)\end{aligned}$$

The substitution of Eq. (4.27) and the trigonometric properties of Eq. (4.28), allow us to reduce Eq. (4.25) for long time :

$$\frac{d}{dt}\langle l^2\rangle(t) = e^{-\alpha t}\frac{d}{dt}[\theta''_k(t)-\psi''_k(t,0)] + \alpha 4V^2\int_0^t dt' e^{-\alpha(t-t')} \times cos[\mathscr{E}_0(\eta(t)-\eta(t'))] \quad (4.29)$$

If the initial density matrix is site diagonal, $\theta''_k(t)=\psi''_k(t,0)$, Eq. (4.29) simplifies more, and has the final form:

$$\frac{d}{dt}\langle l^2\rangle(t) = 4V^2\int_0^t dt' e^{-\alpha(t-t')}cos[\mathscr{E}_0(\eta(t)-\eta(t'))] \quad (4.30)$$

For a sinusoidal electric field, $f(t)=cos(\omega t)$ and $\eta(t)=sin(\omega t)/\omega$:

$$\langle l^2\rangle(t)-\langle l^2\rangle(0) = 4V^2\int_0^t dt'\int_0^{t'} dt'' e^{-\alpha(t'-t'')}cos[(\mathscr{E}_0/\omega)(sin(\omega t')-sin(\omega t''))] \quad (4.31)$$

This equation cannot be solved analytically. Therefore, we will continue by plotting the MSD as a function of time for different values of the ratios α/ω and $\alpha/\mathscr{E}_0$, using the numerical results of the solution of Eq.(4.31). We used a lattice, of 150 sites and we set the nearest-neighbor intersite interactions V to 0.1. In Figure 4.1 we can see, again that the main behavior of MSD is proportional to time. The initially localized particle diffuses through time, and escapes to infinity.

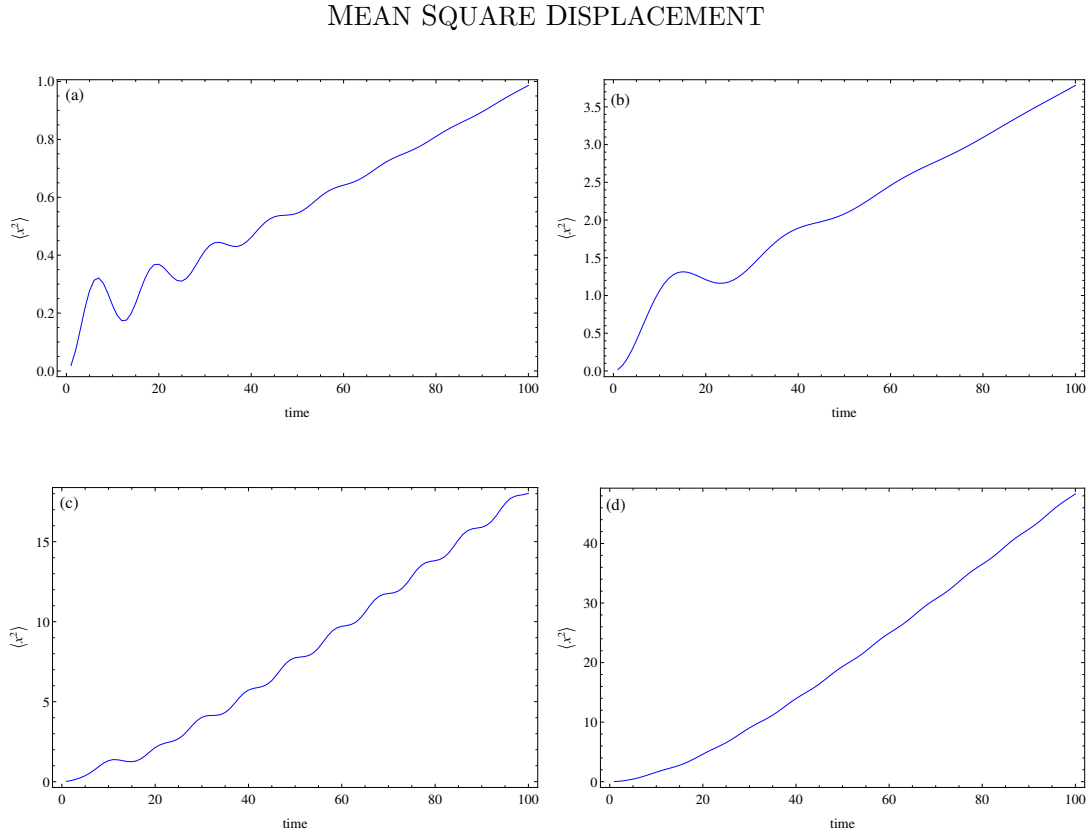

Figure 4.1: The mean square displacement, plotted as a function of time. (a) $\alpha/\omega = 15$ and $\alpha/\mathscr{E}_0 = 0.1$, (b) $\alpha/\omega = 15$ and $\alpha/\mathscr{E}_0 = 0.2$, (c) $\alpha/\omega = 0.15$ and $\alpha/\mathscr{E}_0 = 0.1$, and (d) $\alpha/\omega = 0.15$ and $\alpha/\mathscr{E}_0 = 0.2$.The main behavior of MSD is proportional to time.

4.3 1-D Discrete Two-Band Lattice

We consider now the quantum motion of a charged particle e, moving on a 1-D discrete two-band lattice, of sites l ($-\infty < l < \infty$), where we keep the same energy difference 2ϵ, between the two bands of sites. Assuming that in the first band, all sites have a constant on-site energy $-\epsilon$, while in the second one, all sites have a constant on-site energy too, equals to ϵ.

4.3.1 Absence of Electric Field

In this case when the electric field is not present the Tight−Binding Hamiltonian, for an open system becomes:

$$H^0 = V\sum_l |l\rangle\langle l+1| + |l+1\rangle\langle l| + \epsilon\sum_l (-1)^l |l\rangle\langle l| \tag{4.32}$$

Where the extra term $\epsilon\sum_l(-1)^l|l\rangle\langle l|$ denotes each site's (constant) on-site energy. From Eq. (4.6),we get the new form of the SLE.i.e

$$\begin{aligned} i\frac{\partial}{\partial t}\rho_{m,n} &= V(\rho_{m+1,n} + \rho_{m-1,n} - \rho_{m,n+1} - \rho_{m,n-1}) + \epsilon[(-1)^m - (-1)^n]\rho_{m,n} \\ &\quad -i\alpha\rho^{k,q} + i\alpha\sum_m \rho_{m,m}e^{i(k-q)m} \end{aligned} \tag{4.33}$$

This specific SLE, is a more difficult equation from the previous. For this reason, we will study the quantum motion numerically. More precisely, we will provide numerical solution of Eq.(4.33) and use these results to calculate the MSD as a function of time. In Figure 4.2, we show the outcomes of numerical calculations, where we used a lattice, consisted of 150 sites (75 sites per band). Furthermore, we set the nearest-neighbor intersite interactions V to 0.1 and the on-sites' energy ϵ to 0.1 and the strength of the environmental coupling α equal to 0.7.

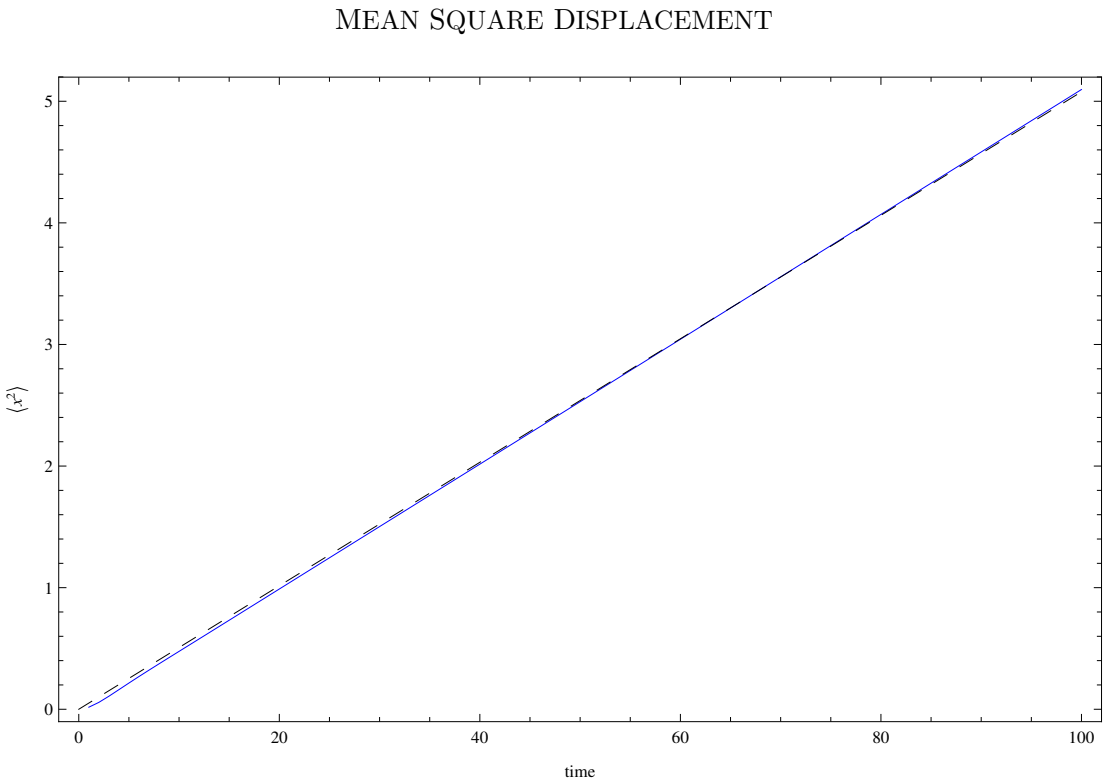

Figure 4.2: The numerical simulation of mean square displacement, plotted as a function of time for the 1-D discrete two-band lattice in the presence of the coupling of the charged particle with the environment($\alpha = 0.5$). We note here, that the MSD $\propto$ t. The blue solid line corresponds to our numerical results and the black dashed line corresponds to best fit of our data.

As we can see, there is no localization and the initially localized particle (at site l=0), delocalized through time , and escapes to infinity, since the MSD is proportional to t. The difference with the MSD in 1-D discrete one-band lattice is the factor, which multiplies the term t. From best fit to our data we find that this factor has the value 0.05 in contrast with the previous section, where that factor had the value 0.08. As we can see, the energy difference between the sites decreases the diffusion.

4.3.2 Presence of Electric Field

Let us consider now, a more complicated case, when the time-dependent electric field is present. As a result, the new Tight-Binding Hamiltonian, has an extra term for the electric field :

$$\begin{aligned} H^0 &= V\sum_l |l\rangle\langle l+1| + |l+1\rangle\langle l| + \epsilon\sum_l (-1)^l |l\rangle\langle l| + \\ &\quad + \mathscr{E}_0 f(t)\sum_l l|l\rangle\langle l| \end{aligned} \tag{4.34}$$

The SLE for this case, now becomes :

$$\begin{aligned} i\frac{\partial}{\partial t}\rho_{m,n} &= V(\rho_{m+1,n} + \rho_{m-1,n} - \rho_{m,n+1} - \rho_{m,n-1}) + \epsilon[(-1)^m - (-1)^n]\rho_{m,n} + \\ &\quad + \mathscr{E}_0 f(t)(m-n)\rho_{m,n} - i\alpha\rho^{k,q} + i\alpha\sum_m \rho_{m,m} e^{i(k-q)m} \end{aligned} \tag{4.35}$$

There is no analytical solution for this SLE. Therefore, we will follow the same procedure by plotting the MSD as a function of time, using our numerical results of the solution of Eq.(4.35). The two-band lattice, is consisted of the same number of sites, furthermore, the nearest-neighbor intersite interactions V, the on-sites' energy ϵ and the strength of the environmental coupling have the same values as before. In the following Figure, (figure 4.3), we have plotted the MSD for different values of the ratios α/ω and $\alpha/\mathscr{E}_0$, for the case of a sinusoidal electric field ($f(t) = cos(\omega t)$), as the ratio $\mathscr{E}_0/V$ was kept constant equal to 5.

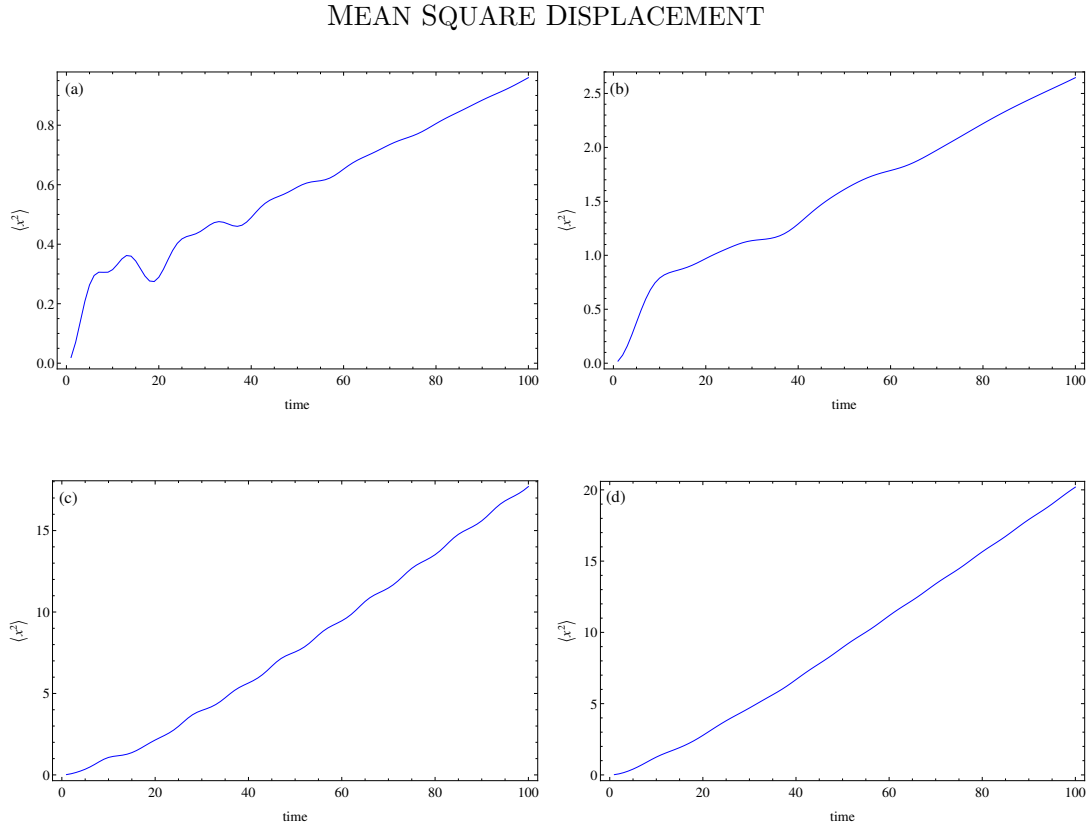

Figure 4.3: The mean square displacement, plotted as a function of time. (a) $\alpha/\omega = 15$ and $\alpha/\mathscr{E}_0 = 0.1$, (b) $\alpha/\omega = 15$ and $\alpha/\mathscr{E}_0 = 0.2$, (c) $\alpha/\omega = 0.15$ and $\alpha/\mathscr{E}_0 = 0.1$, and (d) $\alpha/\omega = 0.15$ and $\alpha/\mathscr{E}_0 = 0.2$.

As one can see, the main behavior for all the different values of the two ratios α/ω and $\alpha/\mathscr{E}_0$ is the same. An initially localized particle, diffuses ($\propto t$) and as a result escapes to infinity.

4.4 1-D Discrete Three-Band Lattice

Now will present the final case for the quantum motion of a charged particle e, on a 1-D discrete three-band lattice, of sites l ($-\infty < l < \infty$). Our lattice consisted by three bands of sites, each doublet of them, has a minimum energy difference ϵ and maximum of 2ϵ. We assume that, in the first band, all sites have constant on-site energy $-\epsilon$, while the second one, has sites with on-site energy equals to 0 and the third one has sites with on-site energy equals to ϵ.

4.4.1 Absence of Electric Field

In the absence of the electric field, we will use again another way to introduce the Tight−Binding Hamiltonian, i.e:

$$H^0 = V \sum_l |l\rangle\langle l+1| + |l+1\rangle\langle l| + \sum_l \epsilon_l |l\rangle\langle l| \tag{4.36}$$

Where now the term $\sum_l \epsilon_l |l\rangle\langle l|$ denotes each site's constant on-site energy, for the three bands $(l, l+1, l+2)$ The SLE for a quantum motion of a charged particle in a discrete three-band lattice, has the following form :

$$\begin{aligned} i\frac{\partial}{\partial t}\rho_{m,n} &= V(\rho_{m+1,n} + \rho_{m-1,n} - \rho_{m,n+1} - \rho_{m,n-1}) + [\epsilon_m - \epsilon_n]\rho_{m,n} \\ &\quad -i\alpha\rho^{k,q} + i\alpha \sum_m \rho_{m,m} e^{i(k-q)m} \end{aligned} \tag{4.37}$$

Our numerical results for this specific quantum motion are presented below, by plotting the MSD as a function of time, where the MSD is calculated using the numerical solution of Eq. (4.37). We set the nearest-neighbor intersite interactions V to 0.1, the on-sites' energy ϵ to 0.1 and the strength of the environmental coupling α equal to 0.5. The next Figure (4.4) of MSD as a function of time, show us that nothing was changed and for the discrete three band lattice. The initially localized particle diffuses proportional to time, and gets delocalized. From best fit to our data we can see that the diffusion in three-band lattice increases in contrast with the previous lattice, since the factor which multiplies the term t is 0.06.

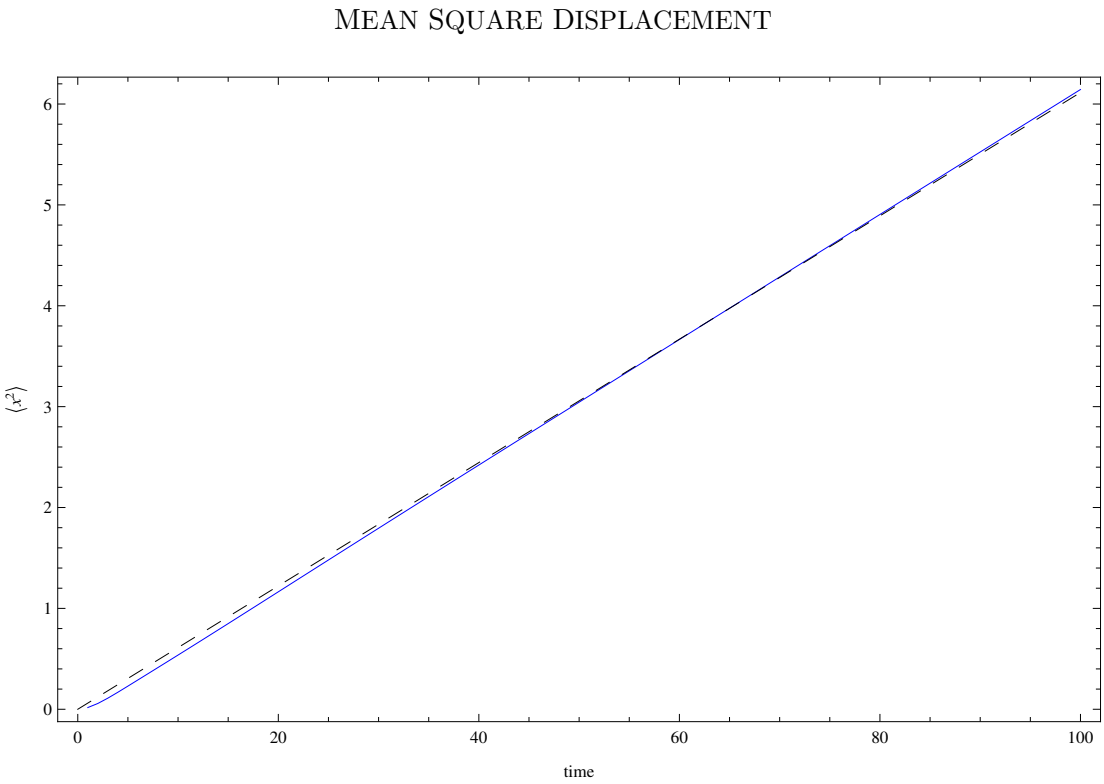

Figure 4.4: The numerical simulation of mean square displacement, plotted as a function of time for the 1-D discrete three-band lattice in the presence of the coupling of the charged particle with the environment. The blue solid line corresponds to our numerical results and the black dashed line corresponds to best fit of our data.

4.4.2 Presence of Electric Field

In the presence of a time-dependent electric field, the time-dependent Tight-Binding Hamiltonian :

$$\begin{aligned} H^0 &= V\sum_l |l\rangle\langle l+1| + |l+1\rangle\langle l| + \sum_l \epsilon_l |l\rangle\langle l| + \\ &\quad + \mathscr{E}_0 f(t) \sum_l l|l\rangle\langle l| \end{aligned} \tag{4.38}$$

The SLE under the presence of a time-dependent electric field becomes :

$$i\frac{\partial}{\partial t}\rho_{m,n} = V(\rho_{m+1,n}+\rho_{m-1,n}-\rho_{m,n+1}-\rho_{m,n-1})+[\epsilon_m-\epsilon_n]\rho_{m,n}+ \\ +\mathscr{E}_0 f(t)(m-n)\rho_{m,n}-i\alpha\rho^{k,q}+i\alpha\sum_m \rho_{m,m}e^{i(k-q)m} \quad (4.39)$$

It follows the figure 4.5, with the MSD as a function of time, α/ω and $\alpha/\mathscr{E}_0$, as in previous sections, for the case of a sinusoidal electric field ($f(t) = cos(\omega t)$), as the ratio $\mathscr{E}_0/V$ was kept constant equal to 5. The three-band lattice, is consisted of the same number of sites and the nearest-neighbor intersite interactions V and the on-sites' energy ϵ. The main behavior of MSD in the presence of the electric field for all graphs remain the same, $\propto t$. The initially localized particle diffuses and escapes to infinity.

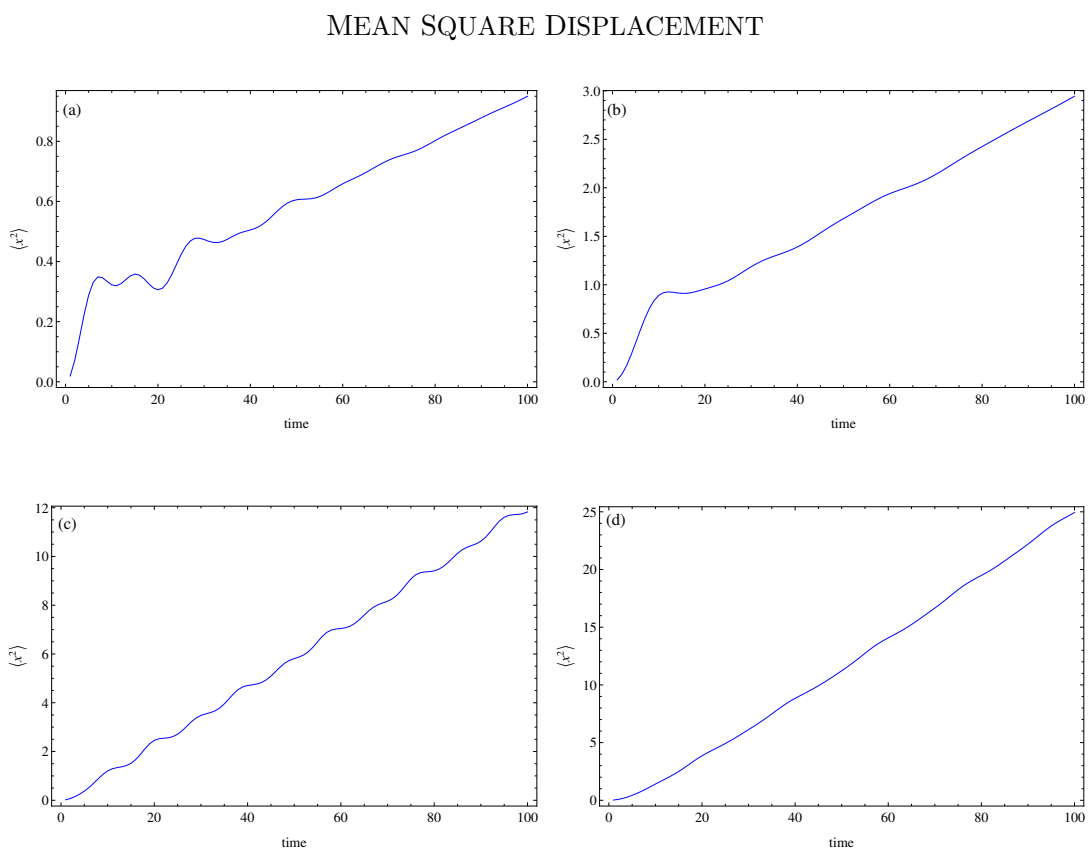

Figure 4.5: The mean square displacement, plotted as a function of time. (a) $\alpha/\omega = 15$ and $\alpha/\mathscr{E}_0 = 0.1$, (b) $\alpha/\omega = 15$ and $\alpha/\mathscr{E}_0 = 0.2$, (c) $\alpha/\omega = 0.15$ and $\alpha/\mathscr{E}_0 = 0.1$, and (d) $\alpha/\omega = 0.15$ and $\alpha/\mathscr{E}_0 = 0.2$.

5 Discussion

The first aim of this work, is to study the classical motion of a Brownian particle in an asymmetric but periodic potential under the influence of an exponentially correlated stochastic time-dependent force, which represented the coupling of the Brownian particle to the environment. This was done by solving the *Langevin equations* (Eq. (2.4)) and calculating numerically the mean value of position (Eq. (2.3)) of the Brownian particle for small and large correlation times (compared to the relaxation time of the system). In the first case we concluded to $\langle x(t)\rangle \to 0$. That was an expected result, since the rates of escape to the left or to the right become equal. As i.e. the correlation time became larger then the mean value of position, is non zero, $\langle x(t)\rangle \neq 0$. In this limit, we can get from the second equation of Eq. (2.4) $\dot{\xi}(t) \approx 0$, in this sense the force which acted in the particle approximately static, i.e. $f + \xi$, although ξ fluctuated but very slowly. When ξ took the appropriate value by canceling the force depended to the potential, the Brownian particle "jumps" to the next well (in our case to the left, but it is not necessary) and so on, as a result we observed the *Brownian ratchet effect*.

We have also examined the quantum motion of a charged particle for three different one-dimensional discrete lattices, (i) one-dimensional discrete one-band lattice, (ii) one-dimensional discrete two-band lattice and (iii) one-dimensional discrete three-band lattice, in the absence/presence of a sinusoidal electric field (for different values

of electric field's frequency (ω) with and without the coupling of the charged particle with the environment. More specifically, we wrote explicitly the Liouville equations for each case, which we solved numerically and for some cases we reproduced the analytical solutions. We used these solutions and we calculated the mean squared displacements, $\langle x^2(t)\rangle$, while the mean displacements, $\langle x(t)\rangle$, for all cases was found to be equal to zero.

In the first case, in the absence of electric field (Eq. (3.9)) the MSD was proportional to t^2, so the particle diffused and escaped to infinity. When we turned on the charged particle coupling with the environment (Eq. (4.7)), once again the initially localized particle diffused, as the MSD was proportional to t. In the presence of the electric field (Eq. (3.23)), when the value $\omega t = 2\pi n$ the MSD was proportional to $J_0^2(\mathscr{E}_0/\omega)t^2$. As a result for any arbitrary value of the ratio $\mathscr{E}_0/\omega$ the MSD increased without bound, while when the ratio took the specific value of the first root of the Bessel function of the first kind, i.e. $\mathscr{E}_0/\omega = 2.405$, where the charged particle remained localized, since the MSD remained bounded. By the interaction of the charged particle with the environment (Eq. (4.20)) the MSD was proportional to t for different values of the ratios $\alpha/\mathscr{E}_0$ and α/ω. When we increased the amplitude of the electric field the rate of diffusion decreased.

For the other two cases, similar diffusion features appeared with a slight difference ,i.e. the diffusion rate decreased as we moved from a discrete one-band lattice to a discrete two-band lattice and then to discrete three-band lattice. When there is no electric field(Eqs (3.49 and (3.53)) the MSD continued to be proportional to t^2, so the particle diffused. When we added the the charged particle coupling with the environment (Eqs (4.33) and (4.37), the initially localized particle diffused (with smaller diffusion rate), as the MSD was again proportional to t. When the electric field was non zero (Eqs (3.49) and (4.39), the MSD increased unbounded ($\propto t^2$), for different values of the ratio $\mathscr{E}_0/\omega$, as a consequence the delocalization of the particle. When the environment came into play, (Eq. (4.35)) the MSD was found to be proportional to t for different values of the ratios $\alpha/\mathscr{E}_0$ and α/ω. Once again, when we increased the amplitude of the electric field the diffusion rate decreased.

Although we treated an open quantum system,no signature of *quantum ratchet effect* was observed. This is because the particular choice of the projection Lindblad operators was such that the environmental coupling with the system was strong enough

to be set to zero very fast, in all the off-diagonal elements of the density matrix. A more suitable choice [20] could be to couple the system with a system of harmonic oscillators, where the environmental terms will remain finite and a possible *quantum ratchet current* could appear.

Bibliography

[1] P. Hänggi and P. Jung, Advances in Chemical Physics **89**, 239-326 (1995) 2

[2] H.P. Breuer and F. Petruccione, *The theory of open quantum systems*, Oxford university press, 2006 3

[3] R. Kubo, J. Phys. Soc. Jpn. **9**, 934 (1954) 3

[4] R.Kubo, *in Fluctuation, Relaxation and Resonance in Magnetic systems*, D.TerHaar, 1962, p.23 3

[5] R. Kubo, J. Math. Phys. **4**, 174 (1963) 3

[6] R. D. Astumian and P. Hänggi, Physics Today **55**, 33-39 (2002) 4

[7] P. Reimann Physics Reports **361**, 57-265 (2002) 4

[8] P. L. Christiansen, M. P. SÃ¸rensen, A. C. Scott, *Nonlinear Science at the Dawn of the 21st Century*, Springer, 2000, pp 357-370 5

[9] T.E. Dialynas and G.P. Tsironis, Phys. Lett. A **218**, 292-296 (1996) 6

[10] T.E. Dialynas, Katja Lindenberg, G.P. Tsironis, Phys. Rev. E **56**, 3976-3985 (1997) 6, 7

[11] V.M. Kenkre and D.W. Brown, Phys. Rev. B **31**, 2479-2487 (1985) 12

[12] I.S. Gradshteyn,I.M. Ryzhik, *Table of integrals Series and Products*, Academic, 1965 16

[13] D.H. Dunlap and V.M. Kenkre, Phys. Rev. B **34**, 3625-3633 (1986) 16

[14] M. Abramowitz and I.A. Stegun, *Handbook of Mathematical Functions*, Dover, 1965 19

[15] V.I. Kovanis and V.M. Kenkre, Phys. Lett. A **130**, 147-150 (1988) 22

[16] Xian-Geng Zhao, J. Phys.: Condens. Matter **9**, 385-390 (1997) 22

[17] Shu-Qing Bao, Xian-Geng Zhao, Xin-Wei Zhang and Wei-Xian Yan Phys. Lett. A **240**, 185-190 (1998) 22

[18] Navinder Singh and N. Kumar, Modern Phys. Let. B **19**, 379-387 (2004) 31

[19] D.H. Dunlap and V.M. Kenkre, Phys. Rev. B **37**, 6622-66313 (1987) 33, 36

[20] R. Roncaglia and G.P. Tsironis, Phys. Rev. Lett. **81**, 1 (1998) 49